Available online at www.sciencedirect.com

ScienceDirect

Advances in Space Research 59 (2017) 1671–1697

ADVANCES IN SPACE RESEARCH (a COSPAR publication)

www.elsevier.com/locate/asr

Review

The Multi-GNSS Experiment (MGEX) of the International GNSS Service (IGS) – Achievements, prospects and challenges

Oliver Montenbruck [a,*], Peter Steigenberger [a], Lars Prange [b], Zhiguo Deng [c], Qile Zhao [d], Felix Perosanz [e], Ignacio Romero [f], Carey Noll [g], Andrea Stürze [h], Georg Weber [i], Ralf Schmid [j], Ken MacLeod [k], Stefan Schaer [l]

[a] Deutsches Zentrum für Luft- und Raumfahrt (DLR), German Space Operations Center (GSOC), 82234 Weßling, Germany
[b] Astronomisches Institut der Universität Bern (AIUB), Sidlerstrasse 5, 3012 Bern, Switzerland
[c] Deutsches GeoForschungsZentrum (GFZ), Telegrafenberg, 14473 Potsdam, Germany
[d] GNSS Research Center, Wuhan University, No. 129 Luoyu Road, Wuhan 430079, China
[e] Centre National d'Etudes Spatiales (CNES), 18, Avenue Edouard Belin, 31401 Toulouse Cedex 9, France
[f] European Space Agency (ESA), European Space Operations Centre (ESOC), Robert-Bosch-Straße 5, 64293 Darmstadt, Germany
[g] Goddard Space Flight Center (GSFC), Code 690.1, Greenbelt, MD 20771, USA
[h] Bundesamt für Kartographie und Geodäsie (BKG), Richard-Strauss-Allee 11, 60598 Frankfurt/Main, Germany
[i] Ntrip Enterprise, Rotdornweg 98, 60433 Frankfurt/Main, Germany
[j] Technische Universität München, Deutsches Geodätisches Forschungsinstitut (DGFI-TUM), Arcisstraße 21, 80333 München, Germany
[k] Canadian Geodetic Survey, Natural Resources Canada (NRCan), 588 Booth Street, Ottawa, Ontario, Canada
[l] Bundesamt für Landestopografie swisstopo, Seftigenstrasse 264, 3084 Wabern, Switzerland

Received 5 November 2016; received in revised form 5 January 2017; accepted 6 January 2017
Available online 17 January 2017

Abstract

Over the past five years, the International GNSS Service (IGS) has made continuous efforts to extend its service from GPS and GLONASS to the variety of newly established global and regional navigation satellite systems. This report summarizes the achievements and progress made in this period by the IGS Multi-GNSS Experiment (MGEX). The status and tracking capabilities of the IGS monitoring station network are presented and the multi-GNSS products derived from this resource are discussed. The achieved performance is assessed and related to the current level of space segment and user equipment characterization. While the performance of orbit and clock products for BeiDou, Galileo, and QZSS still lags behind the legacy GPS and GLONASS products, continued progress has been made since launch of the MGEX project and already enables use of the new constellations for precise point positioning, atmospheric research and other applications. Directions for further research are identified to fully integrate the new constellations into routine GNSS processing. Furthermore, the active support of GNSS providers is encouraged to assist the scientific community in the generation of fully competitive products for the new constellations.

Keywords: IGS; MGEX; BeiDou; Galileo; QZSS; Orbit and clock

* Corresponding author.
E-mail addresses: oliver.montenbruck@dlr.de (O. Montenbruck), peter.steigenberger@dlr.de (P. Steigenberger), lars.prange@aiub.unibe.ch (L. Prange), deng@gfz-potsdam.de (Z. Deng), zhaoql@whu.edu.cn (Q. Zhao), felix.perosanz@cnes.fr (F. Perosanz), ignacio.romero@esa.int (I. Romero), carey.noll@nasa.gov (C. Noll), andrea.stuerze@bkg.bund.de (A. Stürze), georg.weber@ntrip.de (G. Weber), schmid@tum.de (R. Schmid), Ken.MacLeod@NRCan-RNCan.gc.ca (K. MacLeod), Stefan.Schaer@swisstopo.ch (S. Schaer).

http://dx.doi.org/10.1016/j.asr.2017.01.011
0273-1177/

Contents

1. Introduction

The International GNSS Service (IGS; Dow et al., 2009; Johnston et al., 2017) is a volunteer association formed by numerous universities, research institutions, as well as geodetic and space agencies around the globe, which work together to provide highest-quality GNSS data and products on a freely accessible basis for scientific advancement and public benefit. Over the twenty years of its existence, the IGS has continuously advanced the quality of GPS, and later GLONASS, orbit and clock products, thus enabling cutting-edge research and engineering applications.

While one or two global navigation systems may well be considered sufficient for common users, a growing interest in the build-up of independent national positioning, navigation, and timing (PNT) capabilities has triggered a race for new global and regional navigation satellite systems (GNSSs/RNSSs) at the turn of the millennium. The launches of the first Galileo In-Orbit Validation Element (GIOVE) satellite in 2005 and the first test satellite of the Chinese BeiDou-2 constellation (Compass-M1) in 2007 marked the start of a new era in satellite navigation.

Even though remarkable scientific progress has been made (and continues to be made) with legacy GPS and GLONASS observations, the ongoing modernization and the build-up of new constellations offers exciting prospects for further improvement:

- The larger number of satellites and signals-in-space benefits positioning through a reduced dilution of precision (DOP) and offers an improved sky coverage for atmospheric remote sensing from ground (Li et al., 2015a) and space (Harnisch et al., 2013). It also helps to improve the reliability and convergence time for precise point positioning applications (PPP; Tegedor et al., 2014; Li et al., 2015b,c; Ge et al., 2016).
- The availability of unencrypted signals on at least two frequencies and the advanced signal structure of the new GNSSs (Betz, 2016) enables improved tracking performance in terms of precision and robustness with an overall benefit for the availability of measurements. This is of great interest for tracking under severe scintillation but likewise for spaceborne radio occultation (Anthes, 2011) and reflectometry observations (Foti et al., 2015) that are collected at extremely low signal power levels.

- The transmission of triple-frequency signals enables new concepts for signal quality assessment (Simsky, 2006) as well as integer ambiguity resolution in relative navigation and PPP (Teunissen et al., 2002; Ji et al., 2007; Wang and Rothacher, 2013; Tang et al., 2014).
- High-quality clocks onboard the new generations of GNSS satellites enable more accurate inter- and extrapolation of clock offsets with benefits for GNSS radio occultation and real-time PPP (Montenbruck et al., 2012a; Hauschild et al., 2013; Griggs et al., 2015).
- With respect to Earth rotation monitoring and the realization of the global terrestrial reference system, the use of different orbital planes, altitudes and orbital periods of new GNSSs offers an improved diversity. In particular, the non-daily repeat orbits of GLONASS, BeiDou and Galileo may help to reveal systematic effects caused by the 2:1 commensurability of the GPS orbital period and the Earth's rotation (Meindl et al., 2011, 2013; Lutz et al., 2016).

The Cooperative Network for GIOVE Observations (CONGO) built up since 2008 by various German partners (Montenbruck et al., 2009, 2011) provided initial access to new signals and satellites based on the first commercially available multi-GNSS receivers. It enabled an initial characterization and utilization of the modernized GPS and the new Galileo system, and paved the way for a wider recognition of the new constellations in the scientific community. Following the successful examples of the International GLONASS Experiment (IGEX; Willis et al., 1999) and the International GLONASS Service Pilot Project (IGLOS; Weber et al., 2005a), which were conducted to demonstrate the interoperability of GPS and GLONASS and to promote their joint use for scientific applications, the IGS initiated the Multi-GNSS Experiment (MGEX) through a call-for-participation[1] in mid 2011. The call recognized "the availability of new additional GNSS signals and new constellations on the horizon" and aimed at preparing the IGS "for this next phase in the evolution of the IGS to eventually generate products for all GNSS available". The coordination of MGEX-related activities resides within the Multi-GNSS Working Group (Montenbruck and Steigenberger, 2016), which comprises representatives of MGEX data and analysis centers (ACs) as well as selected experts on the subject.

With the build-up of a global and dense multi-GNSS network, MGEX enabled an early familiarization with the diversity of new signals and laid the foundation for a systematic characterization of the new navigation satellite systems. Precise orbit and clock products generated from the observations of the MGEX network have found extensive use in multi-GNSS positioning experiments and other applications. Considering the maturity of the multi-GNSS network and the products already provided by multiple MGEX ACs, the IGS ultimately decided to change the status of MGEX in early 2016. It is now conducted as the "IGS Multi-GNSS Pilot Project" while retaining the well established and widely accepted "trademark" MGEX. Within the coming years, continued efforts will be made to fully integrate all multi-GNSS activities into the regular IGS service portfolio, to offer coherent and transparent access to all existing satellite navigation systems, and to enable their joint use in high-precision science and engineering applications.

The article starts with an overview of new signals made available in the course of GPS/GLONASS modernization and presents the current deployment status of new regional and global navigation systems (Section 2). Subsequently, the evolution and status of the IGS multi-GNSS network are presented in Section 3 along with an overview of the data centers. Orbit and clock products of the new constellations are discussed in Section 4. Aside from an assessment of the achieved performance, specific problems of the orbit, attitude, and measurement modeling are addressed. Section 5 is devoted to signal- and system-related biases, which represent a major conceptual and practical challenge for high-precision multi-GNSS processing. Relevant standards and conventions for multi-GNSS product generation and applications are finally discussed in Section 6, before presenting our summary and conclusions (Section 7).

2. New signals and constellations

2.1. Overview

At the time of writing (October 2016), the GPS constellation is made up of three different blocks of satellites (Table 1). All of them transmit the legacy L1 C/A signal and the encrypted P(Y) signals on L1/L2, which are most widely used by present GPS users. In addition, the new civil L2C signal and the aeronautical L5 signal are broadcast by the more recent generations of Block IIR-M (L2C) and IIF (L2C and L5) satellites. Both signals also carry a new civil navigation message (CNAV) with enhanced content and precision. Even though the availability of three civil signals opens interesting perspectives for, e.g., ambiguity resolution in precise GPS applications, the full potential of triple-frequency navigation is still difficult to realize due to time-varying biases between the L1, L2, and L5 carriers in the Block IIF satellites (Montenbruck et al., 2012b). With a total of 19 L2C-capable satellites and 12 L5-capable satellites, an open dual-frequency service cannot be assured, yet, but availability of a 24-satellite constellation is expected by 2018 and 2024, respectively, after launching an adequate number of GPS III satellites (DOT, 2015). Block IIA satellites that have served as the backbone of the GPS for almost two decades, were finally removed from the constellation in early 2016 (but continue to be available as spare satellites when needed).

[1] ftp://igs.org/pub/resource/pubs/IGS%20M-GEX%20VF.pdf.

Table 1
Status of navigation satellite systems as of October 2016. MEO = medium altitude Earth orbit, IGSO = inclined geosynchronous orbit, GEO = geostationary Earth orbit, IOV = In-Orbit Validation, FOC = Full Operational Capability. Numbers in brackets refer to satellites that have not yet been declared operational or offer restricted functionality.

System	Block	Signals	Satellites
GPS	IIR	L1 C/A, L1/L2 P(Y)	12
	IIR-M	L1 C/A, L1/L2 P(Y), L2C, L1/L2 M	7
	IIF	L1 C/A, L1/L2 P(Y), L2C, L1/L2 M, L5	12
GLONASS	M	L1/L2 C/A & P	23
	M+	L1/L2 C/A & P, L3	1
	K	L1/L2 C/A & P, L3	1+(1)
BeiDou-2	MEO	B1-2, B2, B3	3
	IGSO	B1-2, B2, B3	6
	GEO	B1-2, B2, B3	5+(1)
BeiDou-3	MEO	B1-2, B1, B2, B3ab	2+(1)
	IGSO	B1-2, B1, B2, B3ab	2
Galileo	IOV	E1, E6, E5a/b/ab	3+(1)
	FOC	E1, E6, E5a/b/ab	6+(4)
QZSS	I	L1 C/A, L1C, L1 SAIF, L2C, L6 LEX, L5	1
IRNSS	IGSO	L5/S SPS & RS	4
	GEO	L5/S SPS & RS	3

The GLONASS constellation is mainly composed of GLONASS-M satellites, but already includes one modernized GLONASS-M+ satellite and two GLONASS-K1 satellites. Aside from advanced features such as inter-satellite links, laser time transfer capability and/or improved clocks, the new GLONASS satellites support transmission of the new L3 code division multiple access (CDMA) signal (Urlichich et al., 2011). So far, however, an official interface control document (ICD) is lacking for this signal and availability of a full constellation with L3 capability is unlikely to occur before the end of this decade. Early characterization and utilization of the new GLONASS L3 signal is reported in Zaminpardaz et al. (2016).

Next to GPS and GLONASS, the regional, second-generation BeiDou system (BeiDou-2 or BDS-2) is the third navigation satellite system that has declared an operational service. It is made up of satellites in medium altitude Earth orbit (MEO), inclined geosynchronous orbit (IGSO), and geostationary Earth orbit (GEO). For civil users, BDS-2 offers a signal on the B1-2 side-wing of the B1 band as well as a signal on the B2 (=E5a) band which are fully documented in the open service signal ICD (China Satellite Navigation Office, 2016). Furthermore, an authorized signal on the B3 center frequency can be tracked by various geodetic receivers based on information on the signal modulation and ranging code revealed by high-gain antenna analyses (Grelier et al., 2007; Gao et al., 2009). BeiDou was thus the first system providing triple-frequency signals on all satellites and enabling the validation of triple-frequency navigation algorithms with a full regional constellation.

Shortly after completion of the regional BDS-2 system, China proceeded with the build-up of a global system also known as BeiDou-3 or BDS-3. So far, three MEO and two IGSO satellites have been launched (Tan et al., 2016). Even though no details of the signal structure have been publicly disclosed by the respective authorities, initial observations of the transmitted signals suggest that only the open service B1-2 signal will be inherited for compatibility with BDS-2, while advanced modulations (resembling the planned GPS L1C TM-BOC modulation and the Galileo AltBOC modulation) will be provided on the B1 and B2 (=E5ab) frequencies (Xiao et al., 2016).

The European Galileo system has presently 14 satellites in orbit, which includes 9 satellites providing healthy signals and valid navigation messages as well as two satellites in the commissioning phase. GSAT-104 suffers from a failure of the E5/E6 transmission. GSAT-201 and GSAT-202 have been injected into a wrong orbit and are assigned a "testing" status on the constellation information page of the European GNSS Service Centre[2] While the latter two satellites are unlikely to ever become a part of the operational constellation, they offer proper navigation signals and (most recently) broadcast navigation messages, which allows their use for real-time navigation, PPP and even specific research applications (Delva et al., 2015). Galileo provides an open signal in the E1 band that shares key properties of the future GPS L1C signal as well as a wide-band signal covering the E5ab band. The alternating binary offset carrier (AltBOC) modulation can either be tracked as a composite signal or as distinct signals in the E5a and E5b sub-bands. Since the Galileo E1 and E5a signal frequencies match the L1 and L5 frequencies of GPS, both constellations provide ideal conditions for being treated as a "system of systems" (Hein et al., 2007) in future

[2] https://www.gsc-europa.eu/system-status/Constellation-Information.

GNSS applications. A very first initial service is expected to be declared before the end of 2016 (ION, 2016).

The Japanese Quasi-Zenith Satellite System (QZSS) aims at the build-up of a regional navigation/augmentation service starting with three IGSO satellites and one GEO satellite by 2018. So far, a single Block I satellite (QZS-1, "Michibiki") has been launched in 2010 and is used for testing of signals and services since about six years. The signals transmitted by the QZSS satellites include a basic set of four signals inherited from GPS but using distinct pseudo-random noise (PRN) codes and slightly adapted navigation data. These GPS-compatible signals comprise the L1 C/A, L2C, and L5 signal as well as the L1C signal, which is already used by QZSS but will only be transmitted by the next-generation GPS satellites. In addition, specific signals (L1 Sub-meter class Augmentation with Integrity Function (SAIF), L6 "L-band EXperimental" (LEX)) are broadcast for QZSS augmentation services. Along with the introduction of the new QZSS Block II satellites, a slightly modified/extended set of L5 and L6 signals will be transmitted from 2017 onwards to support the Centimeter Level Augmentation Service and the Positioning Technology Verification Service (Cabinet Office, 2016a,b).

Following China, India is the second nation that has established an independent, regional navigation system. The Indian Regional Navigation Satellite System (IRNSS), which was named NavIC (a Hindi word for boatman and an acronym for Navigation with Indian Constellation) after completion of the seven-satellite constellation, comprises four IGSO and three GEO spacecraft over the Indian ocean region (Harde et al., 2015). While all other systems have so far relied on L-band signals and included an open service signal at or near the GPS L1 frequency, IRNSS is first to employ navigation signals in the S-band along with L5 as the second frequency. Each of these signal frequencies carries signals for the public Standard Positioning Service (SPS) and a Regulated Service (RS). In view of an ever increasing spectral crowding, this choice of signal frequencies clearly improves the "compatibility" with other GNSSs which has been defined as "the ability of global and regional navigation satellite systems and augmentations to be used separately or together without causing unacceptable interference and/or other harm to an individual system and/or service" by the Providers' Forum of the International Committee on Global Navigation Satellite Systems (ICG WGA, 2008). However, it also hampers the support of IRNSS by common GNSS user equipment manufacturers, since S-band signals are clearly incompatible with existing receiver frontends and antenna hardware. It remains to be seen whether market needs will ultimately promote the addition of IRNSS S-band tracking to high-end geodetic receivers.

The summary of current and evolving navigation satellite systems given above offers a first glance at the challenges faced by the IGS and the GNSS user community in fully exploiting the potential benefits of a multi-GNSS world. Compared to standalone GPS, a plethora of new signals on diverse frequencies have emerged, which need to be duly understood and characterized. Many of the new and modernized signals make use of advanced navigation schemes to reduce multipath sensitivity and to improve weak signal tracking capabilities (Betz, 2016). However, aspects such as the availability of distinct pilot and data channels or the use of composite/time-multiplexed BOC modulations offer multiple design options for the "best" tracking mode in a given receiver. These may result in different group and phase delays that need to be understood and calibrated in a proper manner. Early precautions to handle this situation have been made through adoption of the new Version 3 of the Receiver Independent Exchange (RINEX) format for GNSS measurements (IGS RINEX WG and RTCM-SC104, 2015), which allows to distinguish the most important tracking modes (e.g., data-only, pilot-only, or data-plus-pilot) for such types of signals. Nevertheless, this represents only a first step towards the full characterization of user equipment and the development of relevant processing standards.

The vast number of different spacecraft likewise offers substantial challenges for the modeling of geodetic-grade measurements. As discussed further in Section 4, the diversity of attitude control modes and transmit antennas needs to be properly understood to describe the satellite-to-user range at the (sub-) mm-level. In the absence of detailed manufacturer information, extensive research and "reverse-engineering" is often required to achieve that goal.

2.2. Navigation performance

Despite all differences between the individual constellations, an ever increasing stability of atomic frequency standards is common to the new generations of GNSS satellites. Representative performance figures for currently employed satellite clocks are illustrated in Fig. 1, which shows the Allan deviation (ADEV) at time scales of 1–100,000 s.

The latest type of Rubidium atomic frequency standards (RAFSs) employed onboard the GPS IIF satellites (and likewise QZS-1) as well as the passive hydrogen masers (PHMs) used onboard the Galileo satellites exhibit stabilities of $1 - 2 \cdot 10^{-12} \cdot (\tau/\mathrm{s})^{-1/2}$ (Montenbruck et al., 2012a), which is up to ten times better than those of earlier Rubidium and, in particular, Cesium standards. Considering, for example, a time interval of $\tau = 30$ s, an ADEV of $3 \cdot 10^{-13}$ is achieved, which enables short-term clock inter-/extrapolation in PPP with errors down to the few mm level. At time scales of 10,000–100,000 s, Allan deviations as low as $0.5–1 \cdot 10^{-14}$ are obtained. This excellent long-term stability is largely responsible for the low signal-in-space range error (SISRE) of the Galileo and GPS broadcast ephemerides obtained with upload intervals of about 2–24 h.

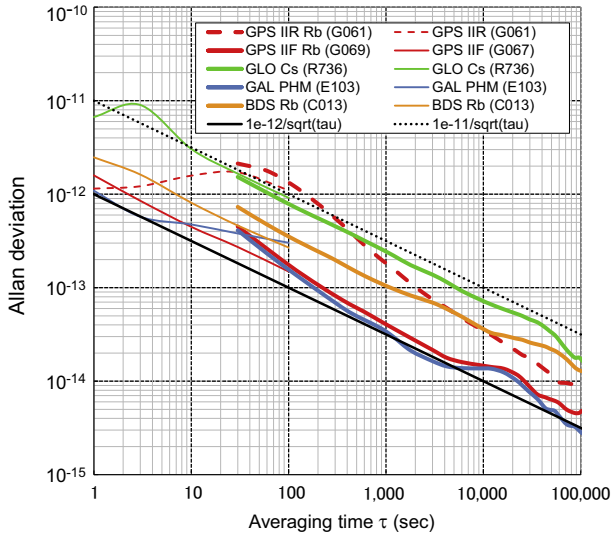

Fig. 1. Stability of atomic frequency standards of selected GNSS satellites as derived from the MGEX orbit and clock product of Deutsches GeoForschungsZentrum (GFZ; Deng et al., 2016) in GPS week 1877 (bold lines; $\tau = 30\,\mathrm{s} \ldots 100,000\,\mathrm{s}$). Complementary values for short time intervals (thin lines; $\tau = 1\,\mathrm{s} \ldots 100\,\mathrm{s}$) were taken from the one-way carrier phase analyses of Griggs et al. (2015). The solid and dotted black lines represent Allan deviations of $10^{-12} \cdot (\tau/\mathrm{s})^{-1/2}$ and $10^{-11} \cdot (\tau/\mathrm{s})^{-1/2}$, respectively. Adapted from Beard and Senior (2017).

A good performance has also been confirmed for the indigenous clocks of the Chinese BeiDou-2 system (see Fig. 1 and Wang et al., 2016a), which show a roughly 3 times larger ADEV than the aforementioned GPS IIF RAFS and the Galileo PHMs. For IRNSS, no independent in-flight characterization has been conducted so far, but a performance of about $5 \cdot 10^{-12} \cdot (\tau/\mathrm{s})^{-1/2}$ can be expected based on the performance of the Galileo RAFS from the same manufacturer.

Broadcast ephemerides (BCEs) transmitted by the GNSS satellites provide orbit and clock information for SPS users. The SISRE is a common quantity to assess the quality of the BCEs by comparison with a precise reference orbit and clock product (Montenbruck et al., 2015a). Whereas precise orbit and clock products refer to the center of mass (CoM) of the satellite, broadcast products refer to the mean antenna phase center. For comparison of both products, the antenna phase center offsets (PCOs) used for the broadcast product generation are needed. However, these PCOs are usually not publicly available. Therefore, Montenbruck et al. (2015a) estimated vertical PCOs from the comparison of broadcast and precise products and used horizontal PCOs from established IGS and MGEX sources. These values are also used here except for the updated GLONASS PCOs listed in Table 2 and the Galileo PCOs listed in Table 3.

SISRE values for August 2016 are presented in Table 4. The MGEX product of GFZ (Uhlemann et al., 2016) is used as a reference as this is the most complete product that is reliably available over the period of interest. The outlier rejection is based on a threshold of 50 m for BDS GEO and 10 m for all other satellites. In addition, Galileo E22 has been excluded on 22 August 2016 from 03:45 to 20:45 due to an anomalous clock behavior.

GPS currently achieves a SISRE of about 60 cm including orbit-only contributions of about 20 cm. Whereas the performance of the GPS CNAV message was initially degraded due to a less frequent update rate compared to LNAV (Steigenberger et al., 2015a), the current CNAV performance is on the same level as LNAV. Although the Galileo orbit SISRE is slightly worse compared to GPS, the total SISRE is significantly smaller (about 40 cm) due to the high stability of the Galileo PHMs. The lower stability of the GLONASS Cesium clocks is responsible for the largest SISRE of more than 2 m. The BeiDou

Table 3
History of Galileo broadcast PCOs. The z-offsets were derived from comparisons with precise products, the horizontal offsets were derived from scale models of the satellites.

Block	Validity	x [cm]	y [cm]	z [cm]
IOV	1/2013–120/2013	−20.0	0.0	165.0
	121/2013–59/2015	−20.0	0.0	85.0
	since 60/2015	−20.0	0.0	75.0
FOC		+15.0	0.0	75.0

Table 4
Signal-in-space range errors for different constellations and navigation messages in August 2016. All values are given in meters. SISRE(orb) denotes the contribution of orbit errors to the range error. LNAV = Legacy Navigation Message, CNAV = Civil Navigation Message, FNAV = Freely accessible Navigation Message, INAV = Integrity Navigation Message.

System	Type	SISRE(orb)	SISRE
GPS	LNAV	0.23	0.56
	CNAV	0.22	0.58
GLONASS		0.59	2.35
Galileo	FNAV	0.27	0.43
	INAV	0.26	0.39
BeiDou	MEO/IGSO	0.82	1.87
	GEO	1.12	2.17

Table 2
GLONASS broadcast PCOs for different types of satellites. z-offsets were determined from comparisons with precise products (August 2016), the horizontal offsets were adopted from igs08.atx.

Block	Satellites	x [cm]	y [cm]	z [cm]
GLONASS-M	SVN 715, 716, 717, 719	−54.5	0.0	245.0
GLONASS-M	SVN 720–747, 851, 853, 854	−54.5	0.0	205.0
GLONASS-M+	SVN 855	−54.5	0.0	205.0
GLONASS-K1	SVN 802	0.0	0.0	165.0

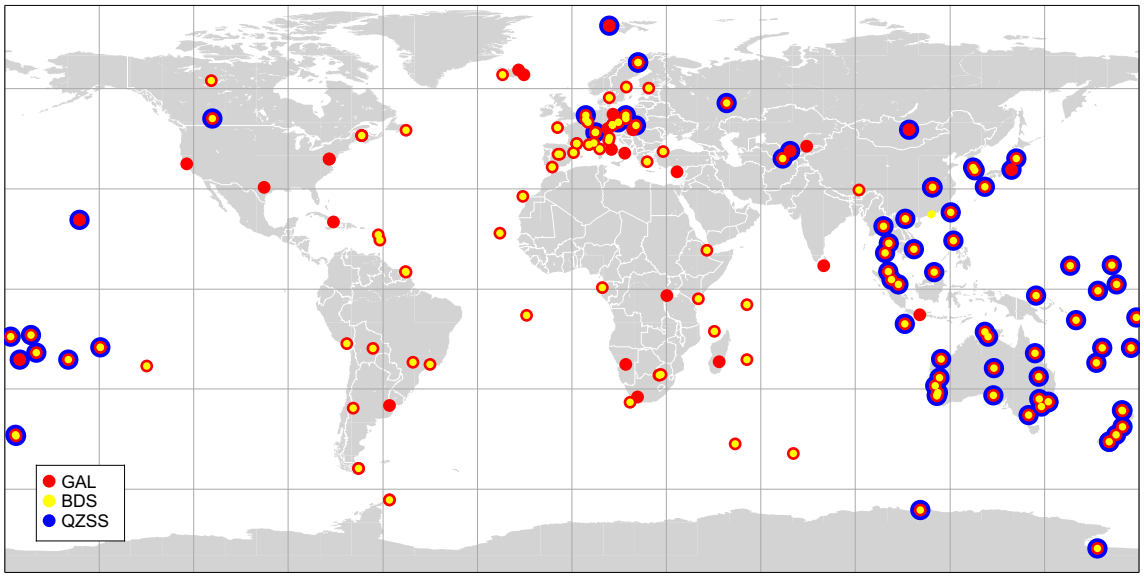

Fig. 2. IGS multi-GNSS stations in October 2016.

Rubidium clocks have a better stability than GLONASS resulting in smaller SISRE values, although the orbit-only SISRE is around 1 m.

Compared to the analyses of Montenbruck et al. (2015a) based on a 12-month dataset from 2013/14, the GPS and Galileo SISREs have improved by 15 cm and 1.2 m, respectively. The GLONASS and BeiDou SISREs show a degradation on the few to several dm level. Whereas the GPS SISRE improvement is mainly related to the decommissioning of old Block IIA satellites, updates of the ground segment led to the significant SISRE improvements for Galileo (Steigenberger and Montenbruck, 2016).

3. The IGS multi-GNSS network and data

Following the MGEX call-for-participation, various institutions started to contribute multi-GNSS observations from newly established or modernized monitoring stations to the IGS. By mid 2012, a small network of about 40 stations with a global, though not yet fully complete, coverage had already emerged. The multi-GNSS network grew rapidly in the following years and comprised about 170 active stations in October 2016. Leading supporters comprise the Centre National d'Etudes Spatiales (CNES) and Institut National de l'Information Géographique et Forestière (IGN), Geoscience Australia (GA), Deutsches GeoForschungsZentrum (GFZ), Japan Aerospace Exploration Agency (JAXA), Deutsches Zentrum für Luft- und Raumfahrt (DLR), Bundesamt für Kartographie und Geodäsie (BKG), and the European Space Agency (ESA), which contribute roughly three quarters of the multi-GNSS stations. A map showing the global distribution of Galileo-, BeiDou- and QZSS-capable stations at this time is given in Fig. 2.

While contributions of new stations for MGEX were initially invited with the primary goal of quickly achieving a good geographic coverage for all new constellations, station quality has been emphasized once the network had grown to an adequate size. By mid 2015, all MGEX stations were formally reviewed for conformity with established IGS site guidelines.[3] These guidelines impose minimum standards (in terms of hardware characteristics, mounting, environment, stability, continuity, etc.) that need to be fulfilled by all IGS stations to support the generation of high quality data and products. With only few exceptions (that were thenceforth treated as "experimental" stations), all previous MGEX stations were fully incorporated into the official IGS network in 2016. Right now, the IGS multi-GNSS stations tracking one or more of the new constellations comprise roughly one third of all 500 IGS stations.[4]

3.1. Station capabilities

The IGS multi-GNSS stations utilize diverse receiver and antenna types from common manufacturers of geodetic-grade GNSS equipment (Javad, Leica, NovAtel, Septentrio, and Trimble). Aside from GPS, GLONASS, and SBAS, all of them support at least one of the new constellations BeiDou, Galileo, and QZSS in two or more frequency bands (Table 5). Even though selected commercial receivers supporting the tracking of IRNSS in the L5 band have recently become available, only very few IGS stations are presently equipped with such receivers. Furthermore, single-frequency tracking alone would neither support the generation of precise orbit and clock products nor enable the use of such stations for PPP.

[3] http://kb.igs.org/hc/en-us/article_attachments/202277487/IGS_Site_Guidelines_July_2015.pdf.

[4] See http://www.igs.org/network.

Table 5
Navigation satellite systems and signals supported by the IGS network (status in October 2016). Signals in parentheses are only tracked by a small subset of receivers.

Constellation	Signals
GPS	L1 C/A & P(Y), L2C & P(Y), L5
GLONASS	L1 C/A & P, L2 C/A & P, L3
BeiDou-2	B1-I, B2-I, B3-I
Galileo	E1 O/S, E5a, E5b, E5ab, (E6)
QZSS	L1 C/A & L1C & SAIF, L2C, L5, LEX
IRNSS	(L5)
SBAS	L1, L5

In addition to the legacy signals on L1 and L2, the IGS multi-GNSS network offers tracking of modernized GPS (L2C, L5), GLONASS (L3), and SBAS (L5) signals. Galileo tracking is supported by almost all multi-GNSS stations resulting in observations on E1, E5a, and E5b as well as the combined E5ab AltBOC signal. Even though the non-public codes transmitted at present have been revealed through in-depth analysis of signal correlations (Yudanov, 2013) and implemented by selected vendors, the unclear future of the commercial service and a possible future encryption of the associated ranging codes (Fernández-Hernández et al., 2015) have so far inhibited a widespread implementation in geodetic receivers. Therefore, only a very limited number of IGS stations presently support Galileo tracking in the E6 band. The Chinese second-generation BeiDou system is supported by roughly half of the network, even though the distribution of stations is not ideally suited to cover the regional constellation. The tracked signals include primarily the open-service signals in the B1-2 and B2 (=E5b) band. Although not defined in the public signal ICD, the tracking of the B3-I signal is, furthermore, supported by a notable fraction of BeiDou-capable stations based on information on the signal structure revealed from high-gain antenna measurements. For QZSS, finally, up to six distinct signals (including the GPS-compatible L1 C/A, L1C, L2C, and L5 signals, as well as the L1 SAIF and L6 LEX signals) are provided by numerous stations in the respective service area.

In contrast to GNSS networks established by various industrial providers of real-time differential correction and point positioning services, the IGS multi-GNSS network is highly heterogeneous due to the diversity of employed receivers, antennas and combinations thereof. While the availability of selected sites with co-located stations and/or receivers connected to a common antenna provides an opportunity for direct comparison of different user equipment, the in-depth characterization of all involved receivers and antennas remains an ongoing challenge for the IGS and its users.

Selected assessments of the tracking performance (noise, multipath, carrier-to-noise density ratio, etc.) using short- and zero-baseline configurations with diverse receivers and antennas have, e.g., been reported by Montenbruck et al. (2011), Odijk and Teunissen (2013), Yang et al. (2014), Cai et al. (2016), and Zaminpardaz et al. (2016) for a variety of new signals. Overall, these analyses demonstrate the benefit of high chipping rates, large spectral bandwidth and increased signal power. Superior performance in terms of noise and multipath can, in particular, be obtained for the Galileo E5ab AltBOC signal (with a 10 MHz chipping rate and a 40 MHz bandwidth), even though these benefits can only partly be materialized when forming an ionosphere-free dual-frequency combination with the lower-grade, open service E1 signal. Furthermore, tracking of this signal is presently lacking for about 20% of the stations of the IGS multi-GNSS network.

Numerous GNSS signals are nowadays located outside the L1/L2 frequency bands used by the legacy GPS and GLONASS signals. All stations designed for multi-GNSS tracking must therefore be equipped with antennas covering essentially the full upper (1559–1610 MHz) and lower L-band (1164–1300 MHz). This is not a problem for newly established sites and stations, but requires due care when upgrading existing IGS stations that contribute to long-time series of geodetic parameters. To minimize discontinuities in the estimated station coordinates and to comply with IGS site guidelines, calibrations of PCOs and phase center variations (PCVs) have therefore been performed by a robotic calibration facility for all new multi-GNSS antenna models prior to their introduction to the IGS network. However, these calibrations are presently confined to GPS and GLONASS L1/L2 frequencies, since live GNSS signals from multiple commonly viewed satellites are required (Schmitz et al., 2002). Nevertheless, these calibrations have enabled the continued use of modernized IGS stations within the routine product generation, which is particularly relevant for stations contributing to the IGS reference frame. As of October 2016, roughly 40 of these stations have already been upgraded for multi-GNSS support, which offers direct access to a common reference frame for all GNSSs.

Some of the legacy IGS stations that have already been upgraded with new multi-GNSS receivers have so far retained their old L1/L2 GPS/GLONASS antennas to avoid discontinuities in geodetic time series. This may result in limitations of the L5 tracking capabilities as well as unusual differential code biases (DCBs) for some of the new signals. Dedicated strategies will have to be developed to transition to real multi-GNSS antennas for these stations without sacrificing the quality of their geodetic products.

3.2. Observation data

Observations from the IGS multi-GNSS network are made available to the users both via IGS data archives and in real-time mode via data streams. While most IGS stations employed for the routine GPS and GLONASS service continue to provide their data in RINEX version 2, MGEX has, from its very beginning, made consequent use of the advanced version 3 standard (IGS RINEX

WG and RTCM-SC104, 2015). This version has been specifically designed to support new constellations with a multitude of diverse signals. In particular, it allows to distinguish different signals and tracking modes that may be used to collect observations on a given frequency. This distinction enables the full consideration of signal- or tracking-mode-specific measurement properties (such as group delays, phase biases and ambiguities) and is thus considered as an important prerequisite for high-precision multi-GNSS data processing.

From the beginning of the Multi-GNSS Experiment, data collected by the MGEX stations have been archived by three IGS data centers, namely the Crustal Dynamics Data Information System (CDDIS; Noll, 2010), IGN, and the GNSS Data Center of BKG. In accord with the specific scope and character of MGEX, all data obtained from the experiment were stored in a dedicated campaign directory[5] rather than the standard IGS data repository.[6] This separation also enabled a clear distinction of multi-GNSS data in RINEX v3 format from legacy GPS/GLONASS data in RINEX v2 format, when stations supported core IGS operations and MGEX in parallel but had to use identical file names for data in the two formats. As a minimum, all multi-GNSS stations are required to deliver daily observation files with a sampling of 30 s. On top of that, hourly 30 s files and/or high-rate data files (1 s sampling, 15 min intervals) are delivered by certain stations.

To preserve the "one network – one archive" strategy of the IGS, a new file naming convention was later adopted as part of the RINEX 3 Transition Plan.[7] The new file names are designed to ensure better transparency and make use of new 9-character station names which extend the old 4-character station names by a monument/marker number, a receiver number and a country code. Further fields identify the data source (data recorded from real-time streams or stored receiver files), start epoch, sampling, duration covered by a RINEX file, and the specific type of data (see Table 6). After the implementation of this naming convention by the individual IGS station providers, multi-GNSS RINEX v3 data (using long filenames) and GPS/GLONASS RINEX v2 data (using short file names) can now be archived in the same directories at the IGS global data centers.

So far, no automated quality control checks are performed on RINEX v3 observation data, but various tools and algorithms (e.g., El-Mowafy, 2015) have already been developed to assess receiver noise, multipath and cycle slips of multi-GNSS measurements. RINEX v3 quality control tools made available to interested users include, e.g., BQC (Liu et al., 2014), G-Nut/Anubis (Vaclavovic and Dousa, 2015), and BNC (Soehne et al., 2015; Weber et al., 2016).

[5] E.g., ftp://cddis.eosdis.nasa.gov/gnss/data/campaign/mgex.

[6] E.g., ftp://cddis.eosdis.nasa.gov/gnss/data/daily.

[7] http://kb.igs.org/hc/en-us/article_attachments/202584007/Rinex_3_transition_plan_v3.0.pdf.

Table 6
RINEX 3 file naming convention according to IGS RINEX WG and RTCM-SC104 (2015). Format: `XXXXMRCCC_K_YYYYDDDHHMM_ddd_sss_tt.FFF.gz` Example: `UNBD00CAN_S_20162150000_01D_30S_MO.crx.gz`.

Field	Description
`XXXX`	4-character IGS station name
`M`	Monument or marker number (0–9)
`R`	Receiver number (0–9)
`CCC`	ISO country code
`K`	Data source: R = from receiver data using vendor or other software S = from data stream (RTCM or other) U = unknown
`YYYY`	4-digit Gregorian year (of nominal start epoch)
`DDD`	3-digit day of year (of nominal start epoch)
`HH`	2-digit hour (of nominal start epoch)
`MM`	2-digit minute (of nominal start epoch)
`ddd`	Nominal duration: 01D = 1 day, 01H = 1 h, 15 M = 15 min
`sss`	Sampling: 30S = 30 s, 01S = 1 s
`tt`	Type of data: GO, RO, EO, JO, CO, IO, SO, MO = GPS, GLONASS, Galileo, QZSS, BDS, IRNSS, SBAS, or mixed observations GN, RN, EN, JN, CN, IN, SN, MN = GPS, GLONASS, Galileo, QZSS, BDS, IRNSS, SBAS, or mixed navigation data MM = meteorological observations
`FFF`	File format: rnx = RINEX crx = Hatanaka compressed RINEX (Hatanaka, 2008)
`gz`	File compression

Besides archived RINEX data, roughly 50% of all IGS multi-GNSS stations also provide real-time data streams, which are distributed through a dedicated BKG caster.[8] In accord with the prevailing standard for the dissemination of GNSS data and differential corrections, the HTTP-based "Networked Transport of RTCM via Internet Protocol" (Ntrip; Weber et al., 2005b) is used for the transmission of IGS multi-GNSS observations (and navigation messages) to MGEX users. Similar to the RINEX format, which provides a receiver-independent standard for non-real-time GNSS data, the latest version 3.3 of the standard for Differential GNSS Services established by the Radio Technical Commission for Maritime Services (RTCM, 2016) defines a vendor- (and constellation-) independent format for encoding observation data from all current GNSSs except for IRNSS.

These so-called Multi Signal Messages (MSMs) are considered as a basis for real-time distribution of multi-GNSS observation data from IGS stations, but are not yet directly supported by most receivers in the IGS network. BKG has therefore implemented a stream conversion service which accepts raw GNSS data in diverse, vendor-specific (and partly proprietary) binary formats and converts them into the RTCM-3 MSM format prior to their distribution to the users (Weber et al., 2011). In this way, multi-GNSS real-

[8] http://mgex.igs-ip.net.

Table 7
BKG real-time streams with broadcast ephemeris data in RTCM 3.2/3.3 format. The bandwidth represents the average data rate over the 5 s repeat interval for transmission of all ephemerides data.

Constellation	Mount point	Messages	Bandwidth
GPS	RTCM3EPH-GPS	1019	3.6 kbps
GLONASS	RTCM3EPH-GLONASS	1020	2.2 kbps
Galileo	RTCM3EPH-GAL	1045, 1046	1.5 kbps
BeiDou	RTCM3EPH-BDS	63	1.7 kbps
QZSS	RTCM3EPH-QZSS	1044	0.1 kbps
SBAS	RTCM3EPH-SBAS	1043	0.5 kbps
Multi-GNSS	RTCM3EPH	all	9.6 kbps

time applications could be developed based on a single, harmonized stream data format from the very beginning of MGEX, even though full implementation of this format at the individual stations is still pending.

Comparable to the IGS real-time service (RTIGS; Caissy et al., 2012), which presently focuses on GPS/GLONASS observation and correction data, the multi-GNSS real-time stations provide their measurements at a 1 Hz data rate. This rate is deemed sufficient for many real-time navigation applications and is mainly motivated by the capabilities of the employed transmission protocol and the commonly available internet bandwidth, but also the receivers employed at the IGS stations. On the other hand, it is evident that specific real-time applications requiring data rates of 10–50 Hz (such as structural monitoring, earthquake and tsunami warning, or scintillation monitoring) are beyond the capabilities of the present IGS multi-GNSS infrastructure.

3.3. Navigation messages

The MGEX multi-GNSS broadcast ephemerides product has been generated by Technische Universität München (TUM) and DLR in a joint effort since 1 January 2013. Real-time streams of currently 38 selected MGEX stations provide the basis for the generation of daily files with the prefix `brdm`.[9] In the beginning, only GPS, GLONASS, and QZSS were covered. Subsequently, additional GNSSs were included: BeiDou since 11 February 2013, SBAS since 3 March 2013, Galileo since 12 March 2013, and IRNSS since 1 January 2016. However, IRNSS BCEs are currently based on the data of only one single receiver contributed by an external provider.

Following a test campaign of the new CNAV message in June 2013, GPS IIR-M and IIF satellites started a pre-operational routine transmission of CNAV on 28 April 2014. CNAV and LNAV data from a global network of 8–10 Javad receivers are provided by DLR and TUM in daily files with the prefix `brdx`[10] in a RINEX-style format (Steigenberger et al., 2015a).

In addition to the broadcast ephemeris files discussed so far, BKG provides a variety of real-time streams with multi-GNSS BCEs at their Ntrip caster.[11] These comprise distinct streams for each individual constellation as well as a combined stream with GPS, GLONASS, Galileo, BeiDou, QZSS, and SBAS ephemerides (Table 7). The BKG ephemeris streams provide complete and timely orbit and clock information for all GNSS satellites in a standardized message format and can serve a variety of applications from real-time positioning services to assisted GNSS.

The streams are generated from about 65 globally distributed real-time stations that provide encoded broadcast ephemerides to the BKG caster. These data are unpacked, decoded, and stored in real-time in a message buffer of most recent ephemeris data for each satellite when passing a basic set of quality and consistency tests (validity interval, position offset w.r.t. previous navigation message, etc.). Based on the accumulated ephemeris parameters, RTCM 3.2/3.3 navigation messages are subsequently generated in real-time and broadcast to the users. As the previous release of this standard (RTCM 3.2 Amendment 2) did not yet cover all required ephemeris types, preliminary message definitions are still employed for SBAS (1043) and BeiDou (63). Navigation messages for each active satellite of a given constellation are transmitted consecutively in the order of ascending PRN or slot number. Data for the full constellation are repeated every 5 s.

According to the overall IGS data policy, all streams are freely available to all users following an initial registration.[12] To facilitate the usage of the binary RTCM messages, all streams can be pulled and decoded with the BKG Ntrip Client (BNC; Weber et al., 2016) which is also made freely available by BKG.[13] Users with near real-time requirements can use BNC for converting broadcast ephemeris streams from RTCM 3.2/3.3 format to RINEX v3.03 navigation files.

4. Orbit and clock products

4.1. MGEX analysis centers

Currently, five ACs generate different sets of products for MGEX:

- Centre National d'Etudes Spatiales (CNES), Collecte Localisation Satellites (CLS).
- Center for Orbit Determination in Europe (CODE).
- Deutsches GeoForschungsZentrum (GFZ).
- Technische Universität München (TUM).
- Wuhan University.

[9] Available at, e.g., ftp://cddis.eosdis.nasa.gov/pub/gps/data/campaign/mgex/daily/rinex3/yyyy/brdm with the 4-digit year `yyyy`.
[10] Available at, e.g., ftp://cddis.eosdis.nasa.gov/pub/gps/data/campaign/mgex/daily/rinex3/yyyy/cnav with the 4-digit year `yyyy`.
[11] http://products.igs-ip.net.
[12] https://register.rtcm-ntrip.org.
[13] https://igs.bkg.bund.de/ntrip/download.

Table 8
Overview of the MGEX analysis center products. For the GBM clock product, only a subset of stations connected to highly stable external clocks is provided with 30 s sampling, whereas the other stations have a 5 min sampling. SP3: orbit and clock product in SP3 format (Hilla, 2016), CLK: clock product in clock RINEX format (Ray and Gurtner, 2010), SNX: variance/covariance information in solution-independent exchange (SINEX) format (Rothacher and Thaller, 2006), ERP: Earth rotation parameters in IERS format (Kouba and Mireault, 1998), BSX: inter-system biases in Bias-SINEX format version 0.01 (Springer, 2011).

Institution	Abbr.	Constellations	SP3	CLK	SNX	ERP	BSX
CNES/CLS	GRM	GPS+GLO+GAL	15 min	30 s	x	–	–
CODE	COM	GPS+GLO+GAL+BDS+QZS	15 min	5 min	–	x	x
GFZ	GBM	GPS+GLO+GAL+BDS+QZS	5 min	30 s	–	x	x
JAXA	QZF	GPS+QZS	5 min	–	–	–	–
TUM	TUM	GAL+QZS	5 min	–	–	–	–
Wuhan Univ.	WUM	GPS+GLO+GAL+BDS+QZS	15 min	5 min	–	x	–

In addition, the final orbit and clock product (QZF) of JAXA[14] is provided to MGEX, which includes both GPS and QZSS information. The products of these ACs are freely available at the IGS data centers of CDDIS[15] and IGN.[16]

CNES/CLS, CODE, GFZ, and Wuhan University also contribute to the IGS operational GPS and GLONASS products. Whereas the CNES/CLS contributions to the IGS final products and to MGEX are extracted from the same solution (Loyer et al., 2016), MGEX-specific solutions are computed by CODE, GFZ, and Wuhan University.

CODE's MGEX contribution (Prange et al., 2016a) includes GPS, GLONASS, Galileo, BeiDou MEO and IGSO as well as QZSS. GFZ (Uhlemann et al., 2016) and Wuhan University (Guo et al., 2016a) in addition also consider the BeiDou GEO satellites. Whereas CNES/CLS, CODE, and GFZ solve for the parameters of the different GNSSs in one step, a two-step approach is applied by TUM (Steigenberger et al., 2011) to generate its Galileo and QZSS products. In a first step, the CODE rapid orbits, clocks, and Earth rotation parameters (ERPs) are used for a GPS-only PPP estimating station coordinates, troposphere zenith delays and gradients, as well as receiver clock offsets. These parameters are kept fixed in the second step solving for Galileo or QZSS orbit and clock parameters as well as inter-system biases. Wuhan University uses a three-step approach with solving for GPS and GLONASS orbit and clock parameters as well as ERPs first. The other two steps are similar to the TUM approach.

The different products of the MGEX ACs are listed in Table 8. All ACs provide orbit and clock estimates in SP3 format with 5–15 min sampling. The availability of individual contributions is shown in Fig. 3. Complementary clock products are made available by four MGEX ACs, but only two of them (CNES/CLS and GFZ) generate a high-rate clock product with 30 s sampling. CNES/CLS also provides full variance/covariance information for station coordinates and ERPs in the solution-independent exchange (SINEX) format (Rothacher and Thaller, 2006). Station-specific inter-system biases of GPS with respect to Galileo/BDS/QZSS as well as station- and satellite-specific inter-frequency biases for GLONASS are provided in a preliminary version of the Bias-SINEX format by CODE and GFZ. The CODE MGEX bias product in addition contains GPS C1P/C1C satellite DCBs. More details on biases are discussed in Section 5.

4.2. Modeling aspects

An overview of processing standards employed by the various MGEX ACs is given in Steigenberger et al. (2015b) and Guo et al. (2017). In the following, selected modeling aspects with particular relevance for the current MGEX products and their performance are discussed.

4.2.1. Attitude

Nominal attitude models covering both yaw-steering (YS) and orbit-normal (ON) modes are described in Montenbruck et al. (2015b) along with block-specific definitions of the spacecraft reference frames. Rather than employing manufacturer-specific axes conventions for each type of spacecraft, an IGS-specific convention has been adopted, in which the $+z$-axis designates the body axis aligned with the antenna boresight, and in which the $+x$-panel is nominally sunlit for all spacecraft using a YS attitude. In this way, a maximum level of compatibility can be achieved in the description of the nominal attitude across all constellations and spacecraft platforms.

The nominal attitude models provide a proper description of the spacecraft orientation outside the eclipse season. However, more elaborate models will be required to describe the attitude profiles during noon and midnight turns at low Sun elevations above the orbital plane as well as YS/ON mode transitions. Efforts to derive the true yaw-angle profile from carrier phase observations have been reported by Hauschild et al. (2012) for QZS-1 as well as Dai et al. (2015) for BeiDou. The employed techniques enable a post-facto analysis of attitude profiles during such events, but have not yet resulted in generic attitude models covering this operational regime.

[14] http://qz-vision.jaxa.jp/USE/en/finalp.
[15] ftp://cddis.eosdis.nasa.gov/pub/gps/products/mgex.
[16] ftp://igs.ign.fr/pub/igs/products/mgex.

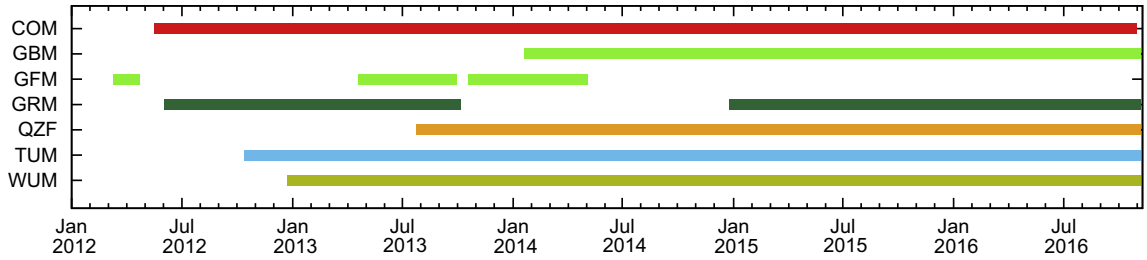

Fig. 3. Availability of MGEX orbit product files. GFM denotes an early GFZ solution considering GPS+GAL that was later discontinued in favor of the GBM product first only including GPS+BDS.

4.2.2. Antenna model

For more than a decade, the IGS has been providing an absolute antenna model with PCOs and PCVs for receiver and satellite antennas. The current model is called igs08.atx (Schmid et al., 2016) and originally contained only legacy GPS and GLONASS frequencies. In mid 2015, satellite antenna PCOs for Galileo, BeiDou, QZSS and IRNSS were added,[17] but zero PCVs were adopted for these systems in the absence of consolidated PCV estimates or calibrations. While PCOs for the two regional systems were made available by the respective system providers, conventional PCOs were initially adopted for Galileo and BeiDou based on the approximate spacecraft body dimensions. More accurate PCO estimates for the Galileo IOV and FOC satellites were derived by Steigenberger et al. (2016) and incorporated into the igs08.atx antenna model in September 2016.[18] For BeiDou, satellite antenna PCOs and PCVs were reported by Dilssner et al. (2014) and Guo et al. (2016a) but are yet too inconsistent to enable an immediate incorporation into the IGS antenna model. For Galileo, QZSS, and IRNSS, the estimation of PCVs is still pending.

For receiver antennas, only L1 and L2 calibrations are contained in the igs08.atx model. While independent PCO/PCV calibrations covering the full frequency range of old and new GNSS signals have been conducted in an anechoic chamber using an artificial signal source (Becker et al., 2010), those calibrations are not yet recommended for multi-GNSS processing due to unexplained discrepancies with robot calibrations for legacy signals (Aerts and Moore, 2013). As a consequence, L2 calibrations are commonly also used for signals in the L5 band. The in-depth characterization and calibration of receiver and satellite antennas therefore remains a continued need for the full integration of new signals and constellations into the IGS service portfolio.

4.2.3. Solar radiation pressure

Solar radiation pressure (SRP) is the largest error source for modeling GNSS satellite orbits. Empirical SRP models estimate suitable parameters that fit the GNSS observation data but do not take into account the physical processes causing these accelerations. A key advantage of these models results from the fact that they can be used for arbitrary GNSS satellites without any a priori knowledge. Disadvantages are the lack of physical interpretation of the estimated parameters and the possible introduction of systematic errors (Rodriguez-Solano et al., 2014).

A widely used example of an empirical SRP model is the Empirical CODE Orbit Model (ECOM-1; Beutler et al., 1994), which considers up to nine parameters in a Sun-oriented reference frame: constant (0), sine (S), and cosine (C) terms in the direction from the satellite to the Sun (D), the solar panel axis (Y), and the direction complementing a right-handed system (B). Usually, only a subset of five parameters (D_0, Y_0, B_0, B_C, B_S) is estimated. Whereas this model performed quite well for GPS satellites, deficiencies were initially identified for GLONASS and later also for Galileo, BDS, and QZSS. Therefore, Arnold et al. (2015) developed ECOM-2 which includes additional estimation terms compared to ECOM-1. ECOM-2 is used by the CODE AC for its MGEX as well as IGS solutions since the beginning of 2015. Prange et al. (2016b) compare the performance of ECOM-1 and ECOM-2 for GPS, GLONASS, Galileo, BeiDou IGSO/MEO, and QZSS. Whereas a clear improvement can be seen for Galileo and QZSS, a degradation is present for BeiDou. However, Prange et al. (2016b) emphasize that both, ECOM-1 and ECOM-2 are strictly designed for satellites in YS mode and thus show clear deficiencies during ON mode of QZSS and BeiDou.

To compensate for the deficiencies of the 5-parameter ECOM-1 in ON mode, Guo et al. (2016a) added a tightly constrained acceleration bias in along-track direction for BeiDou MEO and IGSO satellites. Guo et al. (2016b) showed that this parameterization improves the orbit overlap errors by a factor of about eight during ON mode, although this value is still a factor of two worse compared to YS mode.

Orbit determination of geostationary satellites is particularly challenging due to the static viewing geometry (Wang et al., 2015). As a result, strong correlations between orbital elements, SRP parameters, ambiguities, and DCBs are present. To cope with these correlations, Steigenberger et al. (2013) proposed the estimation of only

[17] See [IGSMAIL-7126], https://igscb.jpl.nasa.gov/pipermail/igsmail/2015/008316.html.
[18] See [IGSMAIL-7356], https://igscb.jpl.nasa.gov/pipermail/igsmail/2016/008546.html.

one SRP parameter in the direction of the Sun. Liu et al. (2016) studied the suitability of different subsets of ECOM-1 parameters and found that a parameterization with D_0, Y_0, B_0, D_S, B_S, and Y_C results in an improved orbit performance compared to the 5-parameter ECOM-1.

Analytical SRP models are based on the dimensions and optical properties of the satellite surfaces. Examples for analytical models of the GPS Block I/II and IIR satellites are given in Fliegel et al. (1992) and Fliegel and Gallini (1996). Rodriguez-Solano (2014) summarizes the dimensions and optical properties of GPS and GLONASS satellites, whereas Guo et al. (2016b) lists a set of values for the BeiDou IGSO and MEO satellites. Unfortunately, such information is not presently available for Galileo, BeiDou GEO, and QZSS satellites. However, purely analytical models are usually not able to model the GNSS observation data with sufficient accuracy. Therefore, empirical parameters can be added to analytical models to improve their performance resulting in a semi-analytical approach.

Rodriguez-Solano et al. (2012a) developed an adjustable box-wing model for GPS satellites that mainly considers the optical properties of the satellite surfaces as well as Y_0 and a rotation lag angle of the solar panels. The orbit overlap and prediction performance of this model is similar to ECOM-1. However, the order of magnitude of the pseudo-stochastic pulses is reduced indicating that the box-wing model allows for a more physical representation of the orbits compared to ECOM-1. In addition, systematic errors at harmonics of the GPS draconitic year in, e.g., station coordinate time series are reduced by the box-wing model (Rodriguez-Solano et al., 2014). Guo et al. (2016b) followed a similar approach for their adjustable box-wing model for BeiDou MEO and IGSO satellites. Whereas the performance of this model is quite similar or only slightly worse compared to ECOM-1 in YS mode, a significantly better accuracy is achieved during ON mode although it is still worse by a factor of about five compared to YS mode.

Montenbruck et al. (2015c) could identify the stretched shape of the Galileo satellite body and the varying cross section as the root cause for systematic errors in Galileo orbits obtained with ECOM-1. They developed an a priori box model for Galileo IOV satellites reducing the peak amplitude of the radial orbit errors from 20 to about 5 cm. However, 5 parameters of ECOM-1 are estimated on top of this model. Steigenberger and Montenbruck (2016) showed that this model is in general also appropriate for Galileo FOC satellites and provided an updated set of model coefficients for this satellite type. Steigenberger et al. (2015c) estimated dedicated box model coefficients for the GIOVE-B satellite and modeled an additional plate that causes shadowing effects. This box-plate model reduced the satellite laser ranging (SLR) offset of GIOVE-B by 10 cm to almost zero. Inspired by Montenbruck et al. (2015c), Zhao et al. (2016) developed an a priori model for QZS-1 reducing the systematic orbit errors in YS and ON mode. In particular, the orbit accuracy improves by a factor of two in ON mode.

4.2.4. Albedo

Albedo or Earth radiation pressure is caused by solar radiation reflected or reemitted by the Earth (Ziebart et al., 2005) and leads to an acceleration that mainly acts in radial direction. As for analytical SRP models, dimensions and optical properties of the satellite are needed for the computation of the albedo acceleration. Modeling of the albedo effect in the precise orbit determination reduces the orbital radius of the GPS Block IIA satellites by about 1 cm (Rodriguez-Solano et al., 2012b). In particular for Galileo, a larger impact on the orbit is expected due to the lower mass compared to GPS. However, due to the uncertain dimensions and optical properties of the satellites, albedo is currently not considered for the new constellations by the majority of MGEX ACs.

4.2.5. Antenna thrust

Antenna thrust is a radial acceleration caused by the transmission of navigation signals by GNSS satellites (Ziebart et al., 2005). For the computation of this acceleration, the total transmit power of the satellite has to be known. Transmit power levels for GPS can be inferred from minimum received signals strength specifications[19] while a value of 100 W is commonly assumed for GLONASS. Rodriguez-Solano et al. (2012b) report a radial effect of about 5 mm for GPS Block IIA satellites. Transmit power levels are currently not available for Galileo, BeiDou, QZSS, and IRNSS. Therefore, this effect is neglected by the MGEX ACs. However, due to the transmission of more signals and the generally lighter satellites, a larger effect of antenna thrust has to be expected compared to the legacy GPS satellites.

4.2.6. Maneuvers

While MEO satellites as used by GPS, GLONASS, and Galileo require only sparse maneuvers to maintain the formation, regular orbit-keeping maneuvers need to be performed by the IGSO and GEO satellites of BDS, QZSS, and IRNSS (Steigenberger et al., 2013; Fan et al., 2017; Montenbruck et al., 2015d).

In the absence of system provider information on the time and magnitude of such maneuvers, a dedicated detection and calibration strategy is employed by the CODE AC (Prange et al., 2016b). In case of obvious discontinuities, orbit solutions for days before and after the event are extrapolated, and the epoch of the closest match is adopted as the effective maneuver time. The strategy has successfully been applied to BDS and QZSS satellites in IGSO, which were found to perform maneuvers roughly twice per year. GFZ detects maneuvers based on the broadcast ephemerides and the data preprocessing. If a maneuver is

[19] See http://acc.igs.org/orbits/thrust-power.txt.

Table 9
RMS values derived from orbit comparisons for the time period 1 January–30 June 2016. All values are given in cm.

	GPS	GLONASS	Galileo		BeiDou			QZSS	
			IOV	FOC	MEO	IGSO	GEO	YS	ON
Radial	1–3	4–11	6–10	4–10	3–11	11–23	54	10–24	30–71
Along-Track	2–4	4–12	10–18	10–19	10–21	24–39	298	28–57	84–133
Cross-Track	2–3	3– 9	9–20	6–14	6–10	17–23	410	16–39	59–156
3D	3–6	6–17	16–29	14–26	12–26	32–51	510	40–73	123–240

detected, the corresponding satellite is excluded from the precise orbit determination (POD) solution. As soon as broadcast ephemerides for the orbit after the maneuver are available, the satellite is considered again. Wuhan University likewise excludes a satellite from their processing, if orbit fitting and the health sign of the navigation message indicate the presence of a maneuver.

4.3. MGEX orbit and clock product quality

A performance assessment of Galileo MGEX products of CNES/CLS, CODE, GFZ, and TUM has previously been performed by Steigenberger et al. (2015b) for a twenty weeks period in mid 2013. They report a general consistency of the orbits of the four ACs at the 5–30 cm level. Guo et al. (2017), furthermore, compared the MGEX products of all ACs for Galileo, BeiDou, and QZSS. They found a consistency of 10–25 cm for Galileo, 10–20 cm, 20–30 cm, and 3–4 m for BeiDou MEO, IGSO, and GEO, respectively, as well as 20–40 cm for QZSS.

In this section, the consistency (precision) of the MGEX orbit products is assessed by orbit comparisons, whereas their accuracy is evaluated by SLR residuals for the first half of 2016. Complementary plots of such quality assessments are made available on the MGEX website[20] with weekly updates. Since users of precise ephemeris products are primarily interested in the combined effect of orbit and clock errors on the modeled code and phase observations, we complement the analyses with an assessment of SISRE values for the various products.

Orbit Comparisons. The consistency of two different orbit products can be evaluated by comparisons of the satellite orbit positions. The minimum and maximum RMS orbit differences for any pair of MGEX ACs are listed in Table 9 for the radial, along-track, and cross-track components as well as the 3D position. Gross outliers exceeding 30 m for BeiDou GEO and 10 m for the other satellites were excluded. For QZSS, time periods with YS and ON are treated separately. Days with QZS-1 attitude switches (16 February and 1 April 2016) and orbit maneuvers (20 April 2016) are excluded. The GPS part of the QZF solution has been excluded due to high 3D RMS values of 9–18 cm that exceed the RMS level of the other ACs by a factor of about four.

Satellite Laser Ranging Residuals. All active BeiDou, Galileo, GLONASS, and QZSS satellites are equipped with laser retroreflector arrays (LRAs; Dell'Agnello et al., 2011) for SLR. Only two GPS Block II satellites (SVN 35 and 36) are equipped with LRAs but these satellites are not active anymore. However, the second batch of GPS III satellites will again carry LRAs. SLR observations can be used for external validation of mainly the radial component of GNSS satellite orbits. SLR range residuals, i.e., the difference between the orbit derived from microwave observations and the distance measured by the optical SLR technique, are used as performance criterion in the following paragraphs.

Whereas all active GLONASS and Galileo satellites are tracked by the International Laser Ranging Service (ILRS; Pearlman et al., 2002), only selected BeiDou satellites are currently considered in accord with the support request of the system provider and the availability of corresponding orbit predictions for ILRS tracking stations. These comprise the MEO satellite M3, the IGSO satellites I3, I5, and I6, and the GEO satellite G1. BeiDou-3 satellites are not considered here, as the IGS multi-GNSS stations do not provide dual-frequency GNSS tracking data for these satellites at the moment.

The SLR residual analysis was performed with DLR's GNSS high precision orbit determination software tools (GHOST; Wermuth et al., 2010). SLR station coordinates are fixed to SLRF2008 (Pavlis, 2009) and ocean tidal loading is corrected for with the FES2004 model (Lyard et al., 2006). Gross outliers exceeding 2 m for BDS GEO, 1 m for BDS IGSO and QZSS, and 0.5 m for all MEO satellites are excluded. All 24 satellites of the nominal GLONASS constellation are considered. For Galileo, the different generations of satellites are analyzed separately: Galileo IOV (GSAT-101–103) and Galileo FOC (GSAT-201–206, 208, 209). BDS-I6 is only included in the GBM solution for about 6 weeks. Offsets and standard deviations (STDs) for the analysis period 1 January until 30 June 2016 are listed in Table 10 for the various MGEX ACs. The number of normal points of the new constellations for this same time interval is shown in Fig. 4. Due to their limited visibility, the GEO and IGSO satellites are in general tracked by 5 and 5–10 stations, only. MEO tracking is performed by 22–24 ILRS stations for BeiDou and Galileo IOV and 15–24 stations for Galileo FOC.

Signal-In-Space Range Error. Similar to the performance analysis of broadcast ephemerides, the SISRE can

[20] http://mgex.igs.org/analysis.

Table 10
SLR residual offsets and standard deviations for the time period 1 January–30 June 2016. All values are given in cm.

	GLONASS	Galileo		BeiDou			QZSS
		IOV	FOC	MEO	IGSO	GEO	
COM	0.5 ± 5.0	−4.3 ± 4.5	−3.5 ± 4.3	−3.4 ± 6.5	−2.8 ± 14.5		−2.0 ± 26.0
GBM	1.0 ± 5.5	−1.7 ± 8.0	−3.0 ± 8.2	−0.3 ± 3.5	−1.1 ± 6.5	−44.7 ± 42.0	15.4 ± 26.5
GRM	0.2 ± 5.2	−0.3 ± 4.5	−1.3 ± 4.7				
QZF							−13.8 ± 16.2
TUM		−6.1 ± 8.8	−4.6 ± 8.6				8.1 ± 28.9
WUM	1.0 ± 5.4	−2.0 ± 4.2	−6.2 ± 9.0	−2.5 ± 4.2	−3.4 ± 8.2	−37.7 ± 29.2	13.1 ± 25.8

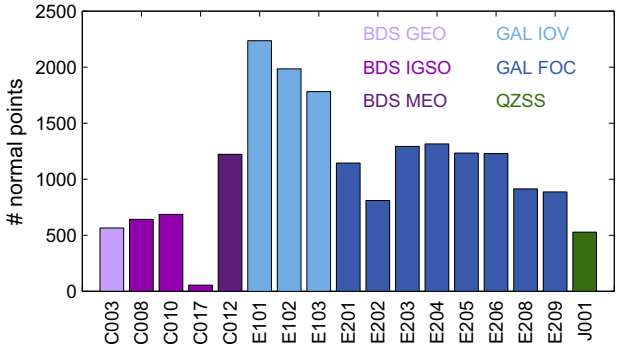

Fig. 4. Number of SLR normal points of the new satellite navigation systems for the time period 1 January–30 June 2016 as used for the analysis in Table 10. Satellites are identified by their space vehicle number (SVN).

be used as a performance indicator for the consistency of precise orbit and clock products. Using the same techniques as applied in Section 2.2 and by Montenbruck et al. (2015a), we obtain global-average SISRE values for a pair of MGEX products of two ACs from a weighted average of the along-track, cross-track and radial orbit differences as well as the clock differences. A common system time difference is removed by subtracting the constellation mean clock difference at each epoch. Since the two products used in the computation are roughly of similar quality, the SISRE values obtained from their difference is not a unique quality measure for an individual orbit and clock product. Still, it provides an indicator for the expected single-point positioning (SPP) performance that can be obtained with either of the two products for a given geometric DOP. For carrier phase based PPP, the estimation of phase ambiguities results in a further absorption of orbit and clock errors, so that the SISRE values reported here may be considered as a conservative performance indicator. Actual PPP results using new constellations may indeed provide better positioning accuracy than suggested by the values compiled in the Tables 11–14.

4.3.1. GPS and GLONASS

While quality-controlled GPS and GLONASS solutions are a well-established part of the IGS service portfolio, the majority of MGEX products listed in Table 8 also include orbit and clock information for these constellations as part

Table 11
SISRE from comparison of precise GPS orbit and clock products of two MGEX ACs for the time period 1 January–30 June 2016. Values in the upper right triangle provide the combined SISRE including orbit and clock differences, while values in the lower left triangle provide the orbit-only contribution SISRE(orb). All values are given in cm. Individual products are identified by 3-letter acronyms indicating the respective ACs (cf. Table 8).

	COM	GBM	GRM	QZF	WUM
COM	–	2.1	1.9	6.2	1.8
GBM	2.5	–	1.4	6.2	1.4
GRM	2.5	2.1	–	4.9	1.1
QZF	5.8	5.6	5.4	–	2.8
WUM	2.2	1.3	2.0	3.4	–

Table 12
SISRE (top right) and SISRE(orb) of MGEX GLONASS products for 1 January–30 June 2016. All values are given in cm. See Table 11 for further explanations.

	COM	GBM	GRM	WUM
COM	–	6.1	7.7	5.5
GBM	4.2	–	4.8	6.5
GRM	4.1	3.7	–	6.7
WUM	5.1	2.0	5.1	–

Table 13
SISRE (top right) and SISRE(orb) of MGEX Galileo products for 1 January–30 June 2016. All values are given in cm. See Table 11 for further explanations.

	COM	GBM	GRM	TUM	WUM
COM	–	3.9	4.9	5.0	3.6
GBM	9.2	–	4.7	5.1	3.1
GRM	6.5	7.5	–	7.4	6.6
TUM	7.4	7.3	8.7	–	5.3
WUM	7.4	7.0	6.8	7.4	–

Table 14
SISRE (top right) and SISRE(orb) of MGEX BeiDou products for 1 January–30 June 2016. All values are given in cm. See Table 11 for further explanations. The values in brackets for the GBM/WUM comparison refer to the complete BeiDou constellation including GEOs, whereas the other values refer to MEO and IGSO satellites only.

	COM	GBM	WUM
COM	–	6.6	6.8
GBM	17.5	–	4.3 (27.4)
WUM	18.5	8.1 (32.1)	–

of a combined multi-GNSS solution. The 3D orbit precision for GPS is mostly at the few cm level (Table 9), and the SISRE is confined to 1–3 cm (Table 11). As an exception, the QZF product shows a slightly degraded performance of about 6 cm in comparison to other solutions. For GLONASS, the individual products exhibit a consistency at the 5–15 cm level (3D RMS orbit difference) and SISRE values of about 5 cm (Tables 9 and 12). The GLONASS SLR residuals with a bias of up to 1 cm and a STD of about 5 cm are slightly worse than the results reported in Sośnica et al. (2015). With the exception of QZF, the consistency of MGEX orbit and clock solutions for GPS and GLONASS is generally found to be at the same level as the standard IGS products.

4.3.2. Galileo

The Galileo orbit products show a consistency at the 15–30 cm level in terms of 3D RMS (Table 9). Differences between IOV and FOC are mainly attributed due to differences in orbit modeling: e.g., both TUM and WUM use ECOM-1 for the FOC satellites yielding the smallest RMS difference in the radial component of about 4 cm. For the IOV satellites, TUM also uses ECOM-1 whereas WUM applies ECOM-2 resulting in the largest radial RMS difference of about 10 cm. This example illustrates that the orbit comparisons have to be interpreted with care as they mainly evaluate the consistency of two solutions. This means that solutions with the same systematic errors of ECOM-1 (TUM and WUM/FOC) can exhibit good consistency but are still not accurate as will be demonstrated later by the SLR residuals. The SISRE values for Galileo are between 3 and 7 cm (Table 13) which is similar to GLONASS. However, the orbit-only SISRE of GLONASS is smaller by a factor of nearly two compared to Galileo.

Orbit differences between individual ACs are largely driven by the use of different SRP models as illustrated in Fig. 5 for the TUM (using ECOM-1) and the CODE solution (using ECOM-2). In the radial direction, a modulation of the orbit differences with peak-to-peak amplitudes between a few cm and up to 40 cm can be seen. The magnitude of this effect depends on the elevation of the Sun above the orbital plane (β-angle) and is common to all Galileo satellites within the same orbital plane. Satellites in other planes typically show similar variations but at different periods of the year. Slightly smaller differences can be observed during the eclipse period indicated by the gray-shaded area in Fig. 5. However, in the middle of the eclipse period, when the β-angle is close to zero, differences with peak-to-peak amplitudes of up to 80 cm occur which can be attributed to the use of different attitude models in this period. In the cross-track direction, a systematic bias of up to 20 cm with an almost semi-annual period can be observed. Similar effects are again encountered for satellites in other orbital planes.

In the SLR analysis (Table 10), two groups of ACs can be distinguished for Galileo: GBM, TUM and WUM/FOC

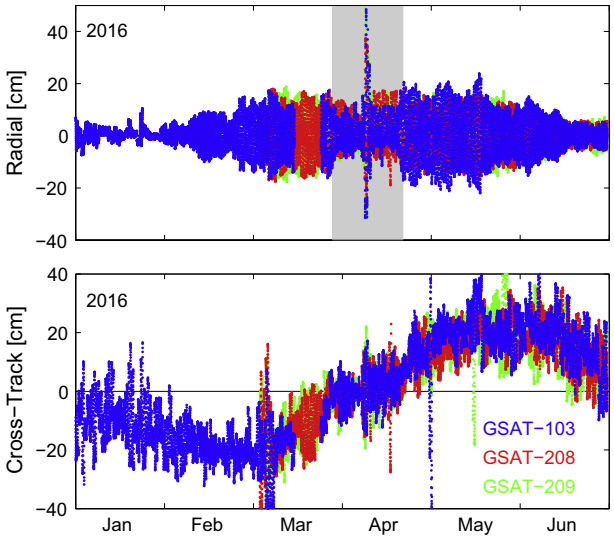

Fig. 5. Orbit differences between COM and TUM for Galileo satellites in orbital plane C. The gray-shaded area indicates the eclipse period.

still use the legacy ECOM-1 model resulting in STDs of about 8 cm. More sophisticated SRP models like ECOM-2 (COM, WUM/IOV) or an a priori box-wing model (GRM) result in STDs of only 4–5 cm. The SLR residual offsets of all ACs are negative and range from almost zero to −6 cm. The neglect of albedo and antenna thrust by most ACs could be an explanation for this systematic bias. As an exception, albedo forces are considered in the GRM product for Galileo IOV and FOC satellites, which results in a slightly larger orbital radius and, thus, reduced SLR biases compared to the other ACs.

4.3.3. BeiDou

Due to their different orbit characteristics and the resulting POD differences, BeiDou MEO, IGSO, and GEO satellites are treated separately in Tables 9 and 10. As already mentioned in Section 4.1, the CODE product does not include BeiDou GEO satellites. The BeiDou MEO satellite orbits show a similar consistency as those of Galileo with 3D RMS values in the range of 12–26 cm. The consistency of the IGSO satellites is about a factor of two worse. For the MEO and IGSO satellites, the GBM/WUM comparison shows the same level of consistency in ON and YS mode. However, the ON mode periods are clearly visible in the COM/GBM and COM/WUM comparisons as this attitude mode is not yet modeled by CODE.

GEO POD solutions exhibit the lowest consistency (about 5 m) as a result of the static viewing geometry which does not allow to determine all orbital elements with similar accuracy. Proposed remedies include tracking from LEO satellites (Guo et al., 2016c) and joint GNSS/SLR POD (Sun et al., 2016) but have not been employed in the routine product generation so far. Considering the full

BeiDou constellation results in a SISRE of about 0.3 m due to the large orbit errors of the GEO satellites (Table 14). Limiting to MEO and IGSO satellites improves the SISRE to 4–7 cm which is similar to Galileo, although the orbit-only SISRE of up to 18 cm is worse by a factor of about two.

Significant differences between the three types of satellites can also be seen in the SLR residuals (Table 10): MEO and IGSO satellites have few cm biases with STDs of 4–7 cm and 7–15 cm, respectively. The BeiDou GEO satellites exhibit a significant bias of about −0.4 m and STDs of 0.3–0.4 m, which may suggest SRP modeling problems in context with the ON mode attitude of these satellites.

4.3.4. QZSS

Due to the significantly different performance during YS and ON mode, these two attitude modes are treated separately for QZSS in Table 9. TUM has been excluded for the YS comparison due to large 3D RMS values of 1.2–1.3 m. The RMS of the other ACs is in the range of 0.4–0.7 m which is a factor of about 1.5 worse compared to the BeiDou IGSO satellites. In ON mode, the consistency degrades by a factor of about three due to generally inappropriate modeling of this special attitude mode. The SLR biases of the different ACs range from −2 cm to +15 cm with STDs of up to 30 cm (Table 10).

4.4. Product combination

At the moment, only MGEX products of individual ACs are available. A combined MGEX product as generated by the IGS Analysis Center Coordinator for the IGS ultra-rapid, rapid, and final orbits and clocks (Kouba and Springer, 2001) is pending for multi-GNSS as well as combined SINEX (Rebischung et al., 2016) and troposphere products (Byram et al., 2011). First trials of a combined GPS+Galileo product are given in Uhlemann et al. (2016) with an agreement of 3–10 cm for the Galileo IOV orbits of CODE, GFZ, and TUM. More recent results of GPS, GLONASS, Galileo, BeiDou, and QZSS for CODE, GFZ, CNES/CLS and Wuhan University are presented in Fritsche (2016). These ACs exhibit weighted root-mean square (WRMS) orbit differences w.r.t. the combined solution of about 5 cm for Galileo, 3–5 cm for BeiDou MEOs in YS mode, 0.1–0.2 m for BeiDou IGSOs, and 1–2 m for BeiDou GEOs. For QZSS, orbit WRMS values of 0.1–0.2 m are achieved during YS mode but can exceed 1 m during ON mode.

Independent experience in multi-GNSS orbit and clock combination has also been gathered in the frame of the international GNSS continuous Monitoring and Assessment System (iGMAS; Echoda et al., 2016; Tan et al., 2016). Chen et al. (2015) present GPS, GLONASS, Galileo, and BeiDou combination results of the iGMAS product integration and service center. For a two week period in 2014, they report WRMS values of about 0.1 m for Galileo, 0.2 m for BeiDou MEO and IGSO, and 1–2 m for BeiDou GEO satellites.

5. Biases

While there is probably no unique and unanimous definition, the term "bias" in the context of GNSS observations usually refers to deviations of the measured value from an idealized reference or a priori model. Biases are commonly treated as additive terms in the functional model of pseudorange and carrier phase observations, and are typically (but not necessarily always) considered as constant values during a given processing arc. Well known examples of GNSS biases include group delays of the satellite signal transmission chain and associated receiver-chain delays, as well as phase biases related to the arbitrary initial phase of the reference oscillator.

Unfortunately, the choice of bias parameters in the observation model is, to a large extent, arbitrary and may vary with the envisaged processing scheme and the desired/accepted model complexity. Furthermore, the actual value of a bias in a specific model will inevitably depend on further definitions and constraints, since the incorporation of bias terms results in a rank-deficient functional model for the observations. By way of example, only the sum of satellite and receiver group delays is accessible to observations (if at all) and a separation of both contributions requires the definition of a "bias-free" reference receiver, the introduction of a zero-mean constraint for a set of satellites, or similar means for removing the rank deficiency. Likewise, the decoupling of biases from clock offset parameters requires the definition of a suitable reference for either of the two. In case of phase biases, only fractional-cycle biases can (or need to) be considered, since it would not be possible to distinguish a potential integer part from the carrier phase ambiguity. Depending on the preferred processing concept, different types of biases become relevant and multiple biases may be lumped into aggregate biases in a different manner. It is therefore paramount to provide a fully transparent description of the employed bias concept when exchanging biases between ACs and users.

The above considerations and concerns apply to all GNSSs and already need to be taken into account in GPS-only processing. They become even more important, though, when introducing multiple constellations and a plethora of different signals into the GNSS processing (Håkansson et al., 2016). Within the following discussion, we focus on DCBs and inter-system biases (ISBs), which have so far been covered most deeply in the literature on new and modernized GNSSs and – in part – already resulted in IGS/MGEX AC products made available to multi-GNSS users and analysts. Specific aspects of phase biases and the problem of half-cycle ambiguities are discussed in Section 5.3.

5.1. Differential code biases

DCBs are well known from GPS (Coco et al., 1991; Yinger et al., 1999) and represent differences in signal travel time for two signals of a given GNSS that are independent of the ionospheric dispersion but rather relate to hardware-dependent group delay differences in the satellite's transmission and the user's reception equipment. Consideration of DCBs in point positioning and timing applications is typically required for single-frequency users, but also for dual-frequency users if the observed pair of signals used to form an ionosphere-free linear combination differs from the one employed in the generation of the GNSS satellite clock offset product (Montenbruck and Hauschild, 2013). Also, DCBs are required as part of ionospheric observations using multi-frequency signals. DCBs are typically caused by frequency-dependent group delays of analog hardware components, but may also occur for signals on a common frequency due to different spectral characteristics of the various modulations. Furthermore, DCBs may originate from differences in the digital signal generation or processing chain.

For practical purposes, DCBs are commonly partitioned into a sum of satellite- and receiver-specific biases. Since the latter can be lumped into the receiver clock offset and are typically ignored in positioning applications, only a limited number of satellite-specific biases needs to be exchanged between ACs and GNSS users. Even though detailed investigations (Aerts et al., 2010; Lestarquit et al., 2012; Vergara et al., 2016) of chip shapes and correlators as well as the transfer function of the entire signal chain reveal that the satellite-plus-receiver DCB cannot be rigorously split into a sum of two independent parts, this treatment still remains a practical necessity despite its approximate character. As shown by Hauschild and Montenbruck (2016), effects are most pronounced for modern receivers using very narrow correlators for multipath mitigation. Here, the use of dedicated receiver-group-specific satellite bias values may be considered as an alternative to the present assumption of receiver-independent satellite biases. While considered as an option in the new Bias-SINEX format (Schaer, 2016) such group-specific biases have not, however, been widely used in practice so far.

With the exception of intra-frequency biases (i.e., DCBs of signals on a common center frequency), the determination of DCBs is necessarily tied to the use of a priori models for the differential ionospheric path delay or the joint estimation of bias and ionosphere parameters. Both methods were employed in recent approaches to multi-GNSS DCB estimation. Global ionosphere maps (GIMs) have been adopted in Montenbruck et al. (2014) as a convenient way of correcting observed pseudorange differences on two signals for the respective ionospheric delay. GIMs provide values of the Vertical Total Electron Content (VTEC) for use with a single-layer mapping function and are routinely generated by various IGS ACs from GPS and GLONASS observations (Hernández-Pajares et al., 2009). While the use of GIMs greatly facilitates the generation of DCBs, it may cause a degraded performance for stations in equatorial regions with pronounced ionospheric variations. The estimation of a local set of ionosphere parameters has therefore been preferred in Wang et al. (2016b) and Xue et al. (2016a,b).

Multi-GNSS DCB products covering a comprehensive set of signals tracked within the IGS network are routinely generated by two ACs (DLR and Chinese Academy of Sciences, CAS) for GPS, GLONASS, BeiDou and Galileo using the aforementioned approaches. They are accessible via the IGS data centers of CDDIS[21] and IGN.[22] It may be noted that QZSS is not presently included in either of the two products, since the availability of just a single satellite prevents the application of a constellation zero-mean constraint. As discussed in Wang et al. (2016b), the two DCB products exhibit a consistency of about 0.2 ns and 0.4 ns for Galileo and BeiDou, respectively. In comparison with established GPS and GLONASS DCB products generated by CODE, the MGEX products exhibit RMS differences of about 0.2 ns and 0.6 ns. These differences can largely be attributed to the use of a new generation of GNSS receivers for the multi-GNSS DCB products, whereas the CODE DCBs are estimated using a larger number of legacy receivers. An overview of DCB values for a selection of relevant signal pairs is shown in Fig. 6. While intra-frequency biases are typically confined to less than ±2 ns for GPS and ±4 ns for GLONASS, inter-frequency biases cover a much wider range of up to 50 ns.

Monthly repeatabilities of the MGEX DCBs are at the 0.1 ns level for GPS and Galileo, and at the 0.2 ns level for BeiDou and GLONASS (Wang et al., 2016b). The inferior stability of GLONASS can largely be attributed to the frequency division multiple access (FDMA) modulation scheme that introduces inter-frequency channel biases not taken into account by the current DCB estimation. The increased scatter of BeiDou DCBs, in contrast, is caused by boresight-dependent group delay variations in the transmit antenna system. As discussed in Wanninger and Beer (2015) and Lou et al. (2017), code and carrier phase observations of BeiDou exhibit a satellite-induced inconsistency that varies with elevation (or, equivalently, the boresight angle) and depends on the signal frequency as well as the satellite type (MEO or IGSO/GEO).

While the exact nature of the BeiDou group delay variation is not yet fully understood, it can in practice be described and corrected by a boresight-angle dependent code phase pattern. Day-to-day DCB variations of BDS satellites can be reduced down to 0.1 ns when using advanced ionosphere estimation concepts in combination with the code phase pattern correction. It is important, though, that consistent code phase patterns are employed

[21] ftp://cddis.eosdis.nasa.gov/pub/gps/products/mgex/dcb.
[22] ftp://igs.ign.fr/pub/igs/products/mgex/dcb.

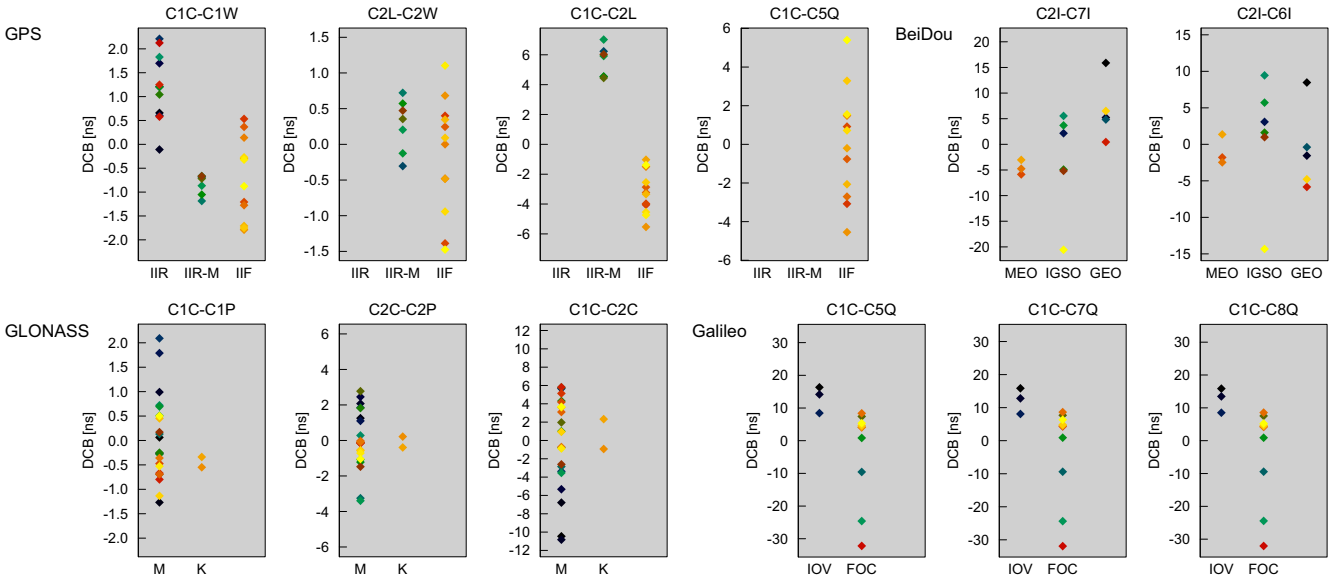

Fig. 6. GNSS satellite DCBs as derived from observations of the IGS multi-GNSS network (mean values for August 2016). Colors distinguish individual spacecraft within the constellation. Columns within each subfigure distinguish individual blocks of satellites. Please note the different scales for the individual DCB values of GPS, GLONASS, and BeiDou. All signals are identified by their corresponding RINEX v3 designations.

in the estimation of DCBs and their subsequent application by the user. This requires establishment of corresponding standards and conventions. For completeness, we also mention that a very good (<0.1 ns) consistence and stability of 7-day and 28-day averages of BDS DCBs has been obtained in Xue et al. (2016b) even without application of a code phase pattern. This apparently positive result can essentially be explained by the 7-day repeat period of the BeiDou constellation but is likely to mask systematic errors related to the choice and distribution of monitoring stations for the DCB determination.

As discussed in Section 2, numerous new GNSS signals provide independent data and pilot channels to their users that require specific attention with respect to DCBs. Pilot channels carry no data modulation, which enables long coherent integration times and increases the robustness at low signal levels or during interference conditions (Betz, 2016). Data channels, in contrast, are used to extract the respective navigation message for real-time positioning. Receiver manufacturers may choose to obtain measurements from tracking either of the components individually or by combining the code correlations of both components into a common tracking loop for increased signal-to-noise ratio.

Examples of pilot/data signals relevant for common users include the I- and Q-channels of the GPS/QZSS L5 and Galileo E5a/E5b signals, the open service components (E1-B and E1-C) of the Galileo E1 signal and, finally, the medium and long component of the GPS/QZSS L2C signal. With the exception of the data and pilot channels of the Galileo E1 open service signal that employ in-phase and anti-phase versions of the composite binary offset carrier (CBOC) modulation and differ slightly in their spectral properties, the data and pilot components of all other signals exhibit strictly identical spectra and should therefore exhibit identical group delays. It remains unclear, though, whether this expectation is actually valid in practice. While the broadcast group delay parameters (BGDs) provided by Galileo as part of its navigation messages do not distinguish between signal components and tracking modes, individual "inter-signal corrections" (ISCs) are provided for the GPS/QZSS L5 I- and Q-components within the CNAV navigation message (GPS Directorate, 2013). On the other hand, only a single ISC parameter is foreseen for the GPS/QZSS L2C-signal, which uses time-multiplexing for the data and pilot component.

The need to distinguish DCBs related to pilot-only, data-only, or data+pilot tracking modes is a matter of ongoing discussion and research within the IGS and the multi-GNSS community in general. For GPS Block IIF satellites, ISCs (i.e. DCBs w.r.t. the L1 P(Y)-code signal) for L5-I5 and L5-Q5 transmitted in the CNAV navigation message differ by up to 7 ns (Fig. 7), even though details of the equipment and methodology used in their determination are not publicly documented.

On the other hand, DCBs for pilot-only tracking (presently employed in Leica, NovAtel and Septentrio multi-GNSS receivers) and combined data+pilot tracking (presently used by Javad and Trimble receivers) as determined within MGEX, exhibit much better consistency. This is illustrated by comparison of GPS L5-minus-L1C/A satellite code biases for pilot-data tracking (designated as $DCB_{C5X-C1C}$ in accord with RINEX v3 signal names) with those for pilot-only tracking (i.e., $DCB_{C5Q-C1C}$). As illustrated in Fig. 8, the $DCB_{C5X-C1C} - DCB_{C5Q-C1C}$ difference exhibits a root-mean-square of 0.4 ns across the entire constellation of Block IIF satellites and day-to-day variations of about 0.1 ns for individual satellites. While not strictly

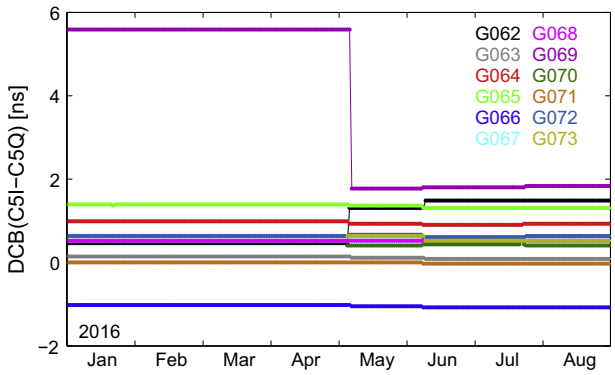

Fig. 7. Difference of inter-signal corrections for L5-I5 and L5-Q5 signals of the GPS Block IIF satellites as transmitted in the CNAV message from Jan. to Aug. 2016. Individual satellites are identified by their SVN.

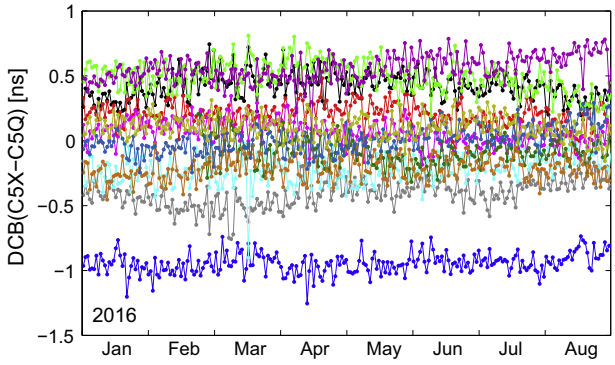

Fig. 8. Difference of $DCB_{C5X-C1C}$ and $DCB_{C5Q-C1C}$ biases for the GPS L5 signal as derived from observations of the IGS multi-GNSS network from Jan. to Aug. 2016. The satellite-specific color codes are the same as in Fig. 7.

compatible, a comparison of Figs. 7 and 8 raises concerns about the quality and applicability of the GPS broadcast ISCs for users in the field. Further transparency in the ISC determination for the GPS control segment will be required to better interpret and potentially improve the respective parameters.

Results of an MGEX DCB analysis for other signals offering distinct pilot/data tracking options are compiled in Table 15. In all cases the variation of bias differences across the constellation clearly exceeds the day-to-day variation of values for individual satellites that indicates the precision of the DCB determination. On the other hand, the differences of DCBs for different tracking modes have not been derived with a common set of receivers, but are potentially masked by characteristics of the two receiver groups. The dependence of "satellite-specific" biases on the receivers used for their estimation has, e.g., been evidenced in Hauschild and Montenbruck (2016) and is also obvious from comparison of DCBs for GPS legacy signals derived with IGS multi-GNSS stations and the old IGS GPS/GLONASS stations (Montenbruck et al., 2014; Wang et al., 2016b). It is also worth noting that the DCB differences between the two tracking modes and/or receiver groups are most pronounced for GPS L5 but less evident for the time-multiplexed GPS L2C signals and the digitally-generated Galileo E5a/b/ab signals. Use of advanced signal generation units offering clean and reproducible chip shapes in future GNSS satellites is therefore deemed important to minimize such intra-signal biases for users.

From a practical point of view, the DCB differences summarized in Table 15 amount to 0.2–0.6 carrier wavelengths and appear of most relevance for near-instantaneous ambiguity resolution, which relies on accurate modeling of code observations. If mainly related to the actual tracking mode but not the particular receiver, a transition of manufacturers to pilot-only tracking may be advisable to harmonize and simplify the GNSS data processing in high-precision applications. Otherwise, individual receiver groups may need to be distinguished by the IGS in the determination of future DCB products.

5.2. Inter-system biases

While DCBs refer to delays between two signals of a common navigation satellite system, inter-system-biases matter when comparing signals from two different GNSS constellations. Simply speaking, an ISB is a correction considered in the pseudorange (and carrier phase) model to align the measurements of one constellation (e.g. Galileo) with that of a reference constellation (e.g., GPS). As discussed in Montenbruck and Hauschild (2013), the ISB lumps receiver- and signal-specific biases with differences in the time systems of individual constellations.

In practice, ISBs are taken into account in dual-frequency point positioning applications by introducing a free adjustment parameter per station for all constellations other than the reference constellation. It is important, though, to note that the estimated ISBs depend not only on the specific receiver and antenna, but vary with the GNSS clock product that defines the system time scales for the individual constellations. Different IGS multi-GNSS products implement different time scales for each constellation and will thus result in different ISB estimates at the user level. Likewise, use of broadcast ephemerides for single point positioning will result in different ISB estimates than use of precise orbit and clock products.

Since broadcast ephemerides reflect the real-time realizations of the GNSS-specific system time scales, the ISBs observed by the user will include the GNSS system time differences (e.g., the GPS-Galileo Time Offset GGTO) in addition to receiver-specific group delay differences for the employed signals. Each of these contributions will typically amount to a few tens of nanoseconds. By way of example, differences of about 20 ns have been obtained for the Galileo-to-GPS ISBs of four different receivers in Gioia and Borio (2016). This scatter is at a similar order of magnitude as the GGTO itself (Defraigne et al., 2013). Dalla Torre and Caporali (2015) investigated ISBs for various European stations using broadcast clocks as well as

Table 15
Difference of DCBs for combined pilot+data tracking and pilot-only tracking from the DLR MGEX DCB product for Jan. to Aug. 2016. Both the standard deviation of DCB differences across the entire constellation and all epochs, as well as the average standard deviation of daily values for individual satellites are provided. Signals are identified by their RINEX v3 names.

GNSS	DCB (pilot+data)	DCB (pilot-only)	difference σ [ns]	day-to-day scatter $\overline{\sigma_{1d}}$ [ns]
GPS	C2X–C1C	C2L–C1C	0.28	0.02
	C5X–C1C	C5Q–C1C	0.42	0.10
Galileo	C5X–C1X	C5Q–C1C	0.23	0.14
	C7X–C1X	C7Q–C1C	0.24	0.14
	C8X–C1X	C8Q–C1C	0.24	0.14

precise clock products and obtained values at the level of 10–100 ns for GPS, Galileo, BeiDou and QZSS in 2013.

As part of the IGS multi-GNSS orbit and clock products, ISBs are also provided by two MGEX ACs (CODE and GFZ). Since the joint estimation of satellite clock offsets and receiver ISBs results in a rank-1 deficiency, an additional constraint is required in the generation of the orbit and clock products. As a result of different strategies (e.g., definition of a zero ISB for a specific station or use of a zero-mean condition over all stations of a network) different ISBs and system time scales are obtained in the multi-GNSS products generated by different ACs. In particular, ISBs are only weakly determined, if the precise orbit and clock determination is driven by carrier phase observations and gives only low weight to pseudorange measurements.

While the ISBs of different products appear inconsistent at first sight, the differences of two products for individual stations are largely compensated by associated differences in the GNSS satellite clock offsets themselves. In a comparison of MGEX Galileo products, Steigenberger et al. (2015b) have, for example identified a 44 ns clock offset difference between two ACs, which matches the corresponding difference in ISBs. As such, ISBs are no "absolute" quantities for a given station but reflect the leveling of the related clock product. Likewise, point positioning users must expect different ISB estimates for their receiver and antenna, when working with different multi-GNSS clock products. Other than, for example, satellite DCBs, the published ISB values are primarily of interest for the inter-comparison of different solutions. They are not, however, required for the positioning itself.

Between-receiver (BR) differences of ISBs for various families of receivers have been investigated by Odijk and Teunissen (2013), Odijk et al. (2016), Paziewski and Wielgosz (2015), and Paziewski et al. (2015) for code and phase observations in a zero-baseline (or short-baseline) testbed. These differences no longer depend on GNSS time scale difference and can be separately determined for each observation type and signal.

BR-ISB differences of code observations reflect analog and digital group delay difference and thus have a similar nature as the code-DCBs. While close to zero for pairs of identical receivers, values of 10–100 ns may arise for pairs of receivers of different brands or types. As discussed in Odijk et al. (2016), calibration of BR-ISBs is, e.g., of interest for relative navigation applications using mixed GNSS constellations. Here, proper knowledge of the BR-ISBs enables a unified treatment of signals on common frequencies from different GNSSs as if they were part of just a single constellation. By constraining the BR-ISB to known values, the degrees of freedom in the positioning problem are reduced with benefit for the resulting dilution of precision and ambiguity fixing rate. Carrier phase BR-ISBs are further discussed in the following sub-section.

5.3. Phase biases

Next to code observations, GNSS carrier phase observations are likewise affected by various forms of biases in the signal transmission or reception equipment. Due to the ambiguous integer cycle count, carrier phase biases are typically treated as fractional cycle biases in undifferenced processing.

When forming between-receiver and between-satellite double-differences of carrier phase observations on the same frequency, the satellite and receiver biases will usually cancel, thus leaving an ambiguity that is an integer multiple of the wavelength irrespective of the involved types of receivers. Precise positioning using GNSS carrier phase observations is largely based on exploiting the integer nature of their double-difference (DD) ambiguities.

However, what holds for differences within a single constellation is not necessarily valid for mixed-constellation carrier phase differences when working with different types/brands of receivers. While integer-valued DD ambiguities are indeed obtained for some combinations of constellations, signals and receivers, half-cycle and even fractional-cycle BR-ISBs have been evidenced in the previously mentioned analyses of Odijk and Teunissen (2013), Odijk et al. (2016), Paziewski and Wielgosz (2015), and Paziewski et al. (2015). Since the ISBs were found to be stable within the noise limits, they can be calibrated and applied as known quantities in the positioning model. In this way, carrier phase observations from different constellations using the same carrier frequency can effectively be processed as if originating from just a single GNSS.

While the occurrence of fractional cycle BR-ISBs for some signals and receiver pairs is not fully explained and examined, the half-cycle biases obtained in other cases may be understood from an inconsistent interpretation of the specified signal structure (e.g., a sign swap of the secondary ranging code) within the individual receiver types.

Further coordination among manufacturers and/or GNSS providers will be required to remove these half-cycle biases in order to achieve consistent integer ambiguities across constellations.

A particularly surprising case of half-cycle DD ambiguities within a single constellation has been encountered for the B1-I and B2-I open service signals of the BeiDou-2 system. As discussed in detail in Nadarajah et al. (2015), the "inter-satellite type biases" relate to the use of different modulations for the BeiDou-2 MEO/IGSO and GEO satellites. While only a single ranging code is used for the GEO satellites (to enable a 500 Hz data stream), the non-GEO satellites employ a 20-bit secondary ranging code. Early receiver implementations that were partly based on pre-ICD signal information had resulted in partly inconsistent signs of the secondary-code among the various types of receivers and ultimately caused the occurrence of half-cycle biases. Following coordination among receiver manufacturers, the problem could essentially be eliminated, but may still affect existing data holdings.

Another type of phase bias that has gained attention in the context of new GNSS signals relates to the consistency of phase observations from multiple carriers. With the availability of two carriers in the lower L-band (e.g. GPS L2 and L5 or BeiDou B2 and B3) two independent ionosphere-free linear combinations can be formed. Their difference represents a geometry- and ionosphere-free triple-frequency linear combination, which is nominally constant except for receiver noise, multipath and possibly phase wind-up. However, notable variations at orbital time scales have been identified for the GPS Block IIF satellites (Montenbruck et al., 2012b). These variations are most pronounced during the eclipse season (where peak-to-peak amplitudes of up to 40 cm or 1.3 ns are attained) and obviously relate to thermal variations in the phase delays of the transmitter chain. While different formulations of bias terms have been applied by various authors to account for inconsistencies of triple-carrier observations in precise point positioning applications (see, e.g., Tegedor and Øvstedal, 2014; Guo et al., 2016d), no harmonized framework has yet been established to exchange and apply information on this type of bias.

6. Standards and conventions

Despite a high level of diversity exercised within the IGS, the provision of highest precision GNSS data and products necessarily requires a minimum set of standards to facilitate a consistent application by the GNSS user community. With the emergence of numerous new constellations, the IGS has therefore actively promoted the extension of legacy data and formats for a full multi-GNSS support.

- As early as 2007, a new version of the Receiver Independent Exchange Format (RINEX v3.00) was developed, which enabled a seamless support of the wealth of new signals that was about to become available with the modernization of GPS and the upcoming Galileo constellation. The latest release, RINEX v3.03 (IGS RINEX WG and RTCM-SC104, 2015), supports all current regional and global navigation satellite systems. Known limitations include the definition of signals for the third-generation BeiDou system that currently lacks a public signal ICD as well as the support of new navigation message types such as GPS/QZSS CNAV and CNAV2.
- With respect to real-time GNSS data, the RTCM SC-104 standard (RTCM, 2016) offers a framework for the encoding of multi-GNSS observation data in close agreement with the RINEX data contents. However, the specification does not yet cover navigation messages for all constellations, and RTCM users must presently cope with missing or preliminary definitions of IRNSS/NavIC and SBAS navigation data messages.
- Multi-GNSS support is also provided in the Special Product 3 (SP3) orbit data format. As of version SP3-d (Hilla, 2016), constellation letters for all GNSSs have been defined, and the earlier limitation in the total number of satellites has been removed by a more flexible encoding. New constellation codes are, furthermore, accepted for the exchange of clock offset values in the RINEX clock format, even though an official update of the corresponding standard for all GNSSs is presently pending.
- Definitions of antenna types and frequency bands for use within the Antenna Exchange format (ANTEX; Rothacher and Schmid, 2010) have been adapted to enable the specification of antenna PCOs and PCVs for new signals and constellations.
- Finally, a new Bias-SINEX standard has been developed (Schaer, 2016) for multi-GNSS biases, which is presently (October 2016) under discussion and awaiting final approval within the IGS. The Bias-SINEX format supports differential and observable-specific biases as well as inter-system biases for all code and phase observations of all signals and constellations.

While the variety of new and updated data formats described above provides a basic framework for the exchange of multi-GNSS-related information, dedicated processing conventions will likewise be required to harmonize the data processing by the various ACs and the application of their products by the users. For GPS, such processing standards have earlier been established by Kouba and Héroux (2001) as well as Kouba (2015), but numerous aspects of multi-GNSS processing are not yet covered in suitable conventions.

The current IGS antenna phase center model igs08.atx comprises PCOs for QZSS and IRNSS provided by the respective system providers, PCOs for Galileo estimated by two different ACs (Steigenberger et al., 2016), and conventional PCOs for BeiDou based on the approximate satellite body dimensions. The inclusion of consolidated

BeiDou PCOs and of PCVs for all new systems is still an open issue. With respect to satellite code-phase patterns (Wanninger and Beer, 2015; Lou et al., 2017) that are required for a proper modeling of BeiDou-2 observations (and, to a lower extent, also other constellations), a standardized handling within the IGS is presently hampered by ANTEX format restrictions. Adequate provisions for incorporating such information into an advanced IGS antenna model will have to be made as part of future standardization efforts.

7. Summary and conclusions

Within the five years since its foundation, the IGS Multi-GNSS Experiment/pilot project has made substantial progress in making new signals and GNSS constellations accessible to a wide range of users in the engineering and science communities. Tracking of multi-GNSS signals has already become an integrated function of the IGS network and data holdings. Initial orbit, clock, and bias products have been made available that support the incorporation of multiple constellations into GNSS-based precise positioning algorithms and applications.

While the performance of present IGS multi-GNSS products is not yet competitive to that of GPS and GLONASS, the potential benefits (but also problems) of multi-GNSS processing have already been experienced by early application developers and users. Much work remains to be done, though, to realize a fully operational multi-GNSS IGS service. Among others, this comprises the following key tasks:

- Calibration of PCOs and PCVs of multi-GNSS satellite and receiver antennas for all supported GNSS signal frequencies and their incorporation into the IGS antenna model.
- Extension of the IGS multi-GNSS network to cover the full set of openly accessible GNSS signals and constellations. In particular, this applies to IRNSS, BeiDou-3 and Galileo E6.
- Establishment and validation of a combined multi-GNSS orbit and clock product including the definition of a common set of clock reference signals for all constellations.
- Full characterization of all GNSS satellite types with respect to attitude modes, antenna phase center positions, and solar radiation pressure perturbations. Open disclosure of high-level spacecraft parameters by the GNSS providers is deemed important to accelerate this process and to avoid cumbersome reverse engineering.
- Establishment and documentation of multi-GNSS processing standards for IGS ACs and users including the harmonization of formulations and products for PPP using undifferenced and uncombined observations.

The implementation of these steps will be pursued by the IGS Multi-GNSS Working Group in close cooperation with other IGS entities and the GNSS user community as well as manufacturers and system providers.

Acknowledgments

The IGS Multi-GNSS Experiment is a team effort that could not have been realized without the help of numerous institutions and individuals. In the first place, we would like to highlight the importance of all station providers contributing to the IGS in general and to MGEX in particular. In essence, they provide the basis of all achievements reported in this publication, even though their significance is frequently underestimated or even ignored. Specific thanks appertain to the IGS Network Coordinator David Maggert for administrating the IGS multi-GNSS network. Likewise, the MGEX project benefits from the persistent effort of all ACs that contribute orbit, clock, and bias products for the new GNSSs and thus pave the way for consequent use of these constellations in future engineering and science applications. All of the above contributions are highly appreciated and valued. In addition, the contribution of the ILRS is gratefully acknowledged. The comprehensive tracking of new-generation GNSS satellites by the ILRS station network has proven to be vital for the analysis of radiometric orbit solutions for these satellites and the continued refinement of GNSS orbit models.

References

Aerts, W., Moore, M., 2013. Comparison of UniBonn and IGS08 Antenna Type Means, 6 Dec. 2013. <http://kb.igs.org/hc/en-us/articles/232231088>.

Aerts, W., Bruyninx, C., Defraigne, P., 2010. Bandwidth and sample frequency effects in GPS receiver correlators. In: 5th ESA Workshop on Satellite Navigation Technologies and European Workshop on GNSS Signals and Signal Processing (NAVITEC), http://dx.doi.org/10.1109/NAVITEC.2010.5707983.

Anthes, R.A., 2011. Exploring Earth's atmosphere with radio occultation: contributions to weather, climate and space weather. Atmos. Meas. Tech. 4, 1077–1103. http://dx.doi.org/10.5194/amt-4-1077-2011.

Arnold, D., Meindl, M., Beutler, G., et al., 2015. CODE's new solar radiation pressure model for GNSS orbit determination. J. Geod. 89 (8), 775–791. http://dx.doi.org/10.1007/s00190-015-0814-4.

Beard, R., Senior, K., 2017. Clocks. In: Teunissen, P.G., Montenbruck, O. (Eds.), Springer Handbook of Global Navigation Satellite Systems. Springer, chap. 5.

Becker, M., Zeimetz, P., Schönemann, E., 2010. Anechoic chamber calibrations of phase center variations for new and existing GNSS signals and potential impacts in IGS processing. In: IGS Workshop 2010, Newcastle.

Betz, J., 2016. Engineering Satellite-Based Navigation and Timing – Global Navigation Satellite Systems, Signals, and Receivers. Wiley-IEEE Press.

Beutler, G., Brockmann, E., Gurtner, W., et al., 1994. Extended orbit modeling techniques at the CODE processing center of the international GPS service for geodynamics (IGS): theory and initial results. Manuscr. Geod. 19 (6), 367–386.

Byram, S., Hackman, C., Tracey, J., 2011. Computation of a high-precision GPS-based troposphere product by the USNO. In: ION GNSS 2011, pp. 572–578.

Cabinet Office, 2016a. Quasi-Zenith Satellite System Interface Specification – Centimeter Level Augmentation Service, IS-QZSS-L6-001, Draft 12 July 2016.

Cabinet Office, 2016b. Quasi-Zenith Satellite System Interface Specification – Positioning Technology Verification Service, IS-QZSS-PTV-001, Draft 12 July 2016.

Cai, C., He, C., Santerre, R., et al., 2016. GLONASS and Galileo. Surv. Rev. 48 (349), 287–295. http://dx.doi.org/10.1179/1752270615Y.0000000032.

Caissy, M., Agrotis, L., Weber, G., et al., 2012. Coming soon – the International GNSS Real-Time Service. GPS World 23 (6), 52–58.

Chen, K., Xu, T., Chen, G., et al., 2015. The orbit and clock combination of iGMAS analysis centers and the analysis of their precision. In: Sun, J. et al. (Eds.), China Satellite Navigation Conference (CSNC) 2015: Volume II, Lecture Notes in Electrical Engineering, vol. 341. Springer, pp. 421–438. http://dx.doi.org/10.1007/978-3-662-46635-3_36.

China Satellite Navigation Office, 2016. BeiDou Navigation Satellite System Signal In Space Interface Control Document, Open Service Signal (Version 2.1).

Coco, D.S., Coker, C., Dahlke, S.R., Clynch, J.R., 1991. Variability of GPS satellite differential group delay biases. IEEE Trans. Aerospace Electron. Syst. 27 (6), 931–938. http://dx.doi.org/10.1109/7.104264.

Dai, X., Ge, M., Lou, Y., et al., 2015. Estimating the yaw-attitude of BDS IGSO and MEO satellites. J. Geod. 89 (10), 1005–1018. http://dx.doi.org/10.1007/s00190-015-0829-x.

Dalla Torre, A., Caporali, A., 2015. An analysis of intersystem biases for multi-GNSS positioning. GPS Solut. 19 (2), 297–307. http://dx.doi.org/10.1007/s10291-014-0388-2.

Defraigne, P., Aerts, W., Cerretto, G., et al., 2013. Advances on the use of Galileo signals in time metrology: calibrated time transfer and estimation of UTC and GGTO using a combined commercial GPS-Galileo receiver. In: Proc. 45th PTTI Systems and Applications Meeting, Bellevue, WA, pp. 256–262.

Dell'Agnello, S., Delle Monache, G.O., Currie, D.G., et al., 2011. Creation of the new industry-standard space test of laser retroreflectors for the GNSS and LAGEOS. Adv. Space Res. 47 (5), 822–842. http://dx.doi.org/10.1016/j.asr.2010.10.022.

Delva, P., Hees, A., Bertone, S., et al., 2015. Test of the gravitational redshift with stable clocks in eccentric orbits: application to Galileo satellites 5 and 6. Class. Quantum Grav. 32 (23), 232003. http://dx.doi.org/10.1088/0264-9381/32/23/232003.

Deng, Z., Fritsche, M., Uhlemann, M., et al., Reprocessing of GFZ multi-GNSS product GBM. In: IGS Workshop 2016, Sydney.

Dilssner, F., Springer, T., Schönemann, E., Enderle, W., 2014. Estimation of satellite antenna phase center corrections for BeiDou. In: IGS Workshop 2014, Pasadena.

DOT, 2015. 2014 Federal Radionavigation Plan, DOT-VNTSC-OST-R-15-01, Department of Defense, Department of Homeland Security, and Department of Transportation, May 2015.

Dow, J.M., Neilan, R.E., Rizos, C., 2009. The International GNSS Service in a changing landscape of Global Navigation Satellite Systems. J. Geod. 83 (3–4), 191–198. http://dx.doi.org/10.1007/s00190-008-0300-3.

Echoda, N.J.A., Mohammed, B., Ganiyu, I.A., et al., 2016. The international GNSS monitoring and assessment service in a multi-system environment. Inside GNSS 11 (4), 48–54.

El-Mowafy, A., 2015. Estimation of multi-constellation GNSS observation stochastic properties using single receiver single satellite data validation method. Surv. Rev. 47 (341), 99–108. http://dx.doi.org/10.1179/1752270614Y.0000000100.

Fan, L., Jiang, C., Hu, M., 2017. Ground track maintenance for BeiDou IGSO satellites subject to tesseral resonances and the luni-solar perturbations. Adv. Space Res. 59 (3), 753–761. http://dx.doi.org/10.1016/j.asr.2016.09.014.

Fernández-Hernández, I., Rodríguez, I., Tobías, G., et al., 2015. Galileo's commercial service: testing GNSS high accuracy and authentication. Inside GNSS 10 (1), 38–48.

Fliegel, H.F., Gallini, T.E., 1996. Solar force modeling of Block IIR Global Positioning System satellites. J. Spacecr. Rockets 33 (6), 863–866. http://dx.doi.org/10.2514/3.26851.

Fliegel, H.F., Gallini, T.E., Swift, E.R., 1992. Global Positioning System radiation force model for geodetic applications. J. Geophys. Res. 97 (B1), 559–568. http://dx.doi.org/10.1029/91JB02564.

Foti, G., Gommenginger, C., Jales, P., et al., 2015. Spaceborne GNSS reflectometry for ocean winds: first results from the UK TechDemoSat-1 mission. Geophys. Res. Lett. 42 (13), 5435–5441. http://dx.doi.org/10.1002/2015GL064204.

Fritsche, M., 2016. Multi-GNSS orbit and clock combination: preliminary results. In: Geohpy. Res. Abstr., vol. 18, EGU2016-7823.

Gao, G.X., Chen, A., Lo, S., et al., 2009. Compass-M1 broadcast codes in E2, E5b, and E6 frequency bands. IEEE J. Sel. Top. Signal Proc. 3 (4), 599–612. http://dx.doi.org/10.1109/JSTSP.2009.2025635.

Ge, Y., Sun, B., Wang, S., et al., 2016. Convergence time analysis of multi-constellation precise point positioning based on iGMAS products. In: Sun, J. et al. (Eds.), China Satellite Navigation Conference (CSNC) 2016 Proceedings: Volume III, Lecture Notes in Electrical Engineering, vol. 390. Springer, pp. 297–306. http://dx.doi.org/10.1007/978-981-10-0940-2_26.

Gioia, C., Borio, D., 2016. A statistical characterization of the Galileo-to-GPS inter-system bias. J. Geod. 90 (11), 1279–1291. http://dx.doi.org/10.1007/s00190-016-0925-6.

GPS Directorate, 2013. Navstar GPS Space Segment/User Segment L5 Interfaces, Interface Specification, IS-GPS-705D, 24 Sep. 2013, Global Positioning Systems Directorate, Los Angeles Air Force Base, El Segundo, CA.

Grelier, T., Dantepal, J., Delatour, A., et al., 2007. Initial observations and analysis of Compass MEO satellite signals. Inside GNSS 2 (4), 39–43.

Griggs, E., Kursinski, E.R., Akos, D., 2015. Short-term GNSS satellite clock stability. Radio Sci. 50 (8), 813–826. http://dx.doi.org/10.1002/2015RS005667.

Guo, J., Xu, X., Zhao, Q., Liu, J., 2016a. Precise orbit determination for quad-constellation satellites at Wuhan University: strategy, result validation, and comparison. J. Geod. 90 (2), 143–159. http://dx.doi.org/10.1007/s00190-015-0862-9.

Guo, J., Chen, G., Zhao, Q., et al., 2016b. Comparison of solar radiation pressure models for BDS IGSO and MEO satellites with emphasis on improving orbit quality. GPS Solut. http://dx.doi.org/10.1007/s10291-016-0540-2.

Guo, J., Zhao, Q., Li, M., et al., 2016d. Enhanced precise orbit determination for BeiDou satellites with FengYun 3C onboard GNSS tracking data. In: IGS Workshop 2016, Sydney.

Guo, F., Zhang, X., Wang, J., Ren, X., 2016d. Modeling and assessment of triple-frequency BDS precise point positioning. J. Geod. 90 (11), 1223–1235. http://dx.doi.org/10.1007/s00190-016-0920-y.

Guo, F., Li, X., Zhang, X., Wang, J., 2017. Assessment of precise orbit and clock products for Galileo, BeiDou, and QZSS from IGS Multi-GNSS Experiment (MGEX). GPS Solut. 21 (1), 279–290. http://dx.doi.org/10.1007/s10291-016-0523-3.

Håkansson, M., Jensen, A.B.O., Horemuz, M., Hedling, G., 2016. Review of code and phase biases in multi-GNSS positioning. GPS Solut. http://dx.doi.org/10.1007/s10291-016-0572-7.

Harde, H., Shahade, M.R., Badnore, D., 2015. Indian regional navigation satellite system. Int. J. Res. in Sci. Eng. 1 (SP1), 36–42.

Harnisch, F., Healy, S.B., Bauer, P., English, S.J., 2013. Scaling of GNSS radio occultation impact with observation number using an ensemble of data assimilations. Mon. Weather Rev. 141 (12), 4395–4413. http://dx.doi.org/10.1175/MWR-D-13-00098.1.

Hatanaka, Y., 2008. A compression format and tools for GNSS observation data. In: Bulletin of the Geographical Survey Institute, vol. 55. <http://www.gsi.go.jp/ENGLISH/Bulletin55.html>.

Hauschild, A., Montenbruck, O., 2016. A study on the dependency of GNSS pseudorange biases on correlator spacing. GPS Solut. 20 (2), 159–171. http://dx.doi.org/10.1007/s10291-014-0426-0.

Hauschild, A., Steigenberger, P., Rodriguez-Solano, C., 2012. Signal, orbit and attitude analysis of Japan's first QZSS satellite Michibiki. GPS Solut. 16 (1), 127–133. http://dx.doi.org/10.1007/s10291-011-0245-5.

Hauschild, A., Montenbruck, O., Steigenberger, P., 2013. Short-term analysis of GNSS clocks. GPS Solut. 17 (3), 295–307. http://dx.doi.org/10.1007/s10291-012-0278-4.

Hein, G.W., Rodriguez, J.A., Wallner, S., et al., 2007. Envisioning a future GNSS system of systems, Part 1. Inside GNSS 2 (1), 58–67.

Hernández-Pajares, M., Juan, J.M., Sanz, J., et al., 2009. The IGS VTEC Maps: a reliable source of ionospheric information since 1998. J. Geod. 83 (3–4), 263–275. http://dx.doi.org/10.1007/s00190-008-0266-1.

Hilla, S., 2016. The Extended Standard Product 3 Orbit Format (SP3-d), 21 Feb. 2016. <ftp://igscb.jpl.nasa.gov/igscb/data/format/sp3d.pdf>.

ICG WGA, 2008. Report of Working Group A: compatibility and interoperability, ICG/WGA/DEC2008, Third Meeting of the International Committee on Global Navigation Satellite Systems (ICG), Pasadena, CA. <http://www.unoosa.org/pdf/icg/2008/icg3/ICG_WGA_DEC2008.pdf>.

IGS RINEX WG, RTCM-SC104, 2015. RINEX – The Receiver Independent EXchange format, Version 3.03, 14 July 2015. <ftp://igs.org/pub/data/format/rinex303.pdf>.

ION, 2016. GNSS program updates: Galileo. Inst. Navig. Quart. Newslett. 26 (2), 22–23.

Ji, S., Chen, W., Zhao, C., et al., 2007. Single epoch ambiguity resolution for Galileo with the CAR and LAMBDA methods. GPS Solut. 11 (4), 259–268. http://dx.doi.org/10.1007/s10291-007-0057-9.

Johnston, G., Riddell, A., Hausler, G., 2017. The International GNSS Service. In: Teunissen, P.G., Montenbruck, O. (Eds.), Springer Handbook of Global Navigation Satellite Systems. Springer, chap. 33.

Kouba, J., 2015. A guide to using International GNSS Service (IGS) products, <http://kb.igs.org/hc/en-us/article_attachments/203088448/UsingIGSProductsVer21_cor.pdf>.

Kouba, J., Héroux, P., 2001. Precise point positioning using IGS orbit and clock products. GPS Solut. 5 (2), 12–28. http://dx.doi.org/10.1007/PL00012883.

Kouba, J., Mireault, Y., 1998. [IGSMAIL-1943] New IGS ERP Format (version 2). <https://igscb.jpl.nasa.gov/pipermail/igsmail/1998/002017.html>.

Kouba, J., Springer, T., 2001. New IGS station and satellite clock combination. GPS Solut. 4 (4), 31–36. http://dx.doi.org/10.1007/PL00012863.

L. Lestarquit, Y. Gregoire, P. Thevenon, Characterising the GNSS correlation function using a high gain antenna and long coherent integration – Application to signal quality monitoring, in: IEEE/ION PLANS 2012, 877–885, http://dx.doi.org/10.1109/PLANS.2012.6236830, 2012.

Li, X., Zus, F., Lu, C., et al., 2015a. Retrieving of atmospheric parameters from multi-GNSS in real time: validation with water vapor radiometer and numerical weather model. J. Geophys. Res. 120 (14), 7189–7204. http://dx.doi.org/10.1002/2015JD023454.

Li, X., Ge, M., Dai, X., et al., 2015b. Accuracy and reliability of multi-GNSS real-time precise positioning: GPS, GLONASS, BeiDou, and Galileo. J. Geod. 89 (6), 607–635. http://dx.doi.org/10.1007/s00190-015-0802-8.

Li, X., Zhang, X., Ren, X., et al., 2015c. Precise positioning with current multi-constellation Global Navigation Satellite Systems: GPS, GLONASS, Galileo and BeiDou. Sci. Rep. 5, 8328. http://dx.doi.org/10.1038/srep08328.

Liu, H., Tang, G., Imparato, D., et al., 2014. BQC: a new multi-GNSS data quality checking toolkit. In: Proc. European Navigation Conference ENC-GNSS 2014, Nederlands Instituut voor Navigatie.

Liu, J., Gua, D., Ju, B., et al., 2016. A new empirical solar radiation pressure model for BeiDou GEO satellites. Adv. Space Res. 57 (1), 234–244. http://dx.doi.org/10.1016/j.asr.2015.10.043.

Lou, Y., Gong, X., Gu, S., et al., 2017. Assessment of code bias variations of BDS triple-frequency signals and their impacts on ambiguity resolution for long baselines. GPS Solut. 21 (1), 177–186. http://dx.doi.org/10.1007/s10291-016-0514-4.

Loyer, S., Perosanz, F., Mercier, F., et al., CNES/CLS IGS Analysis Center: contribution to MGEX and recent activities. In: IGS Workshop 2016, Sydney.

Lutz, S., Meindl, M., Steigenberger, P., et al., 2016. Impact of the arc length on GNSS analysis results. J. Geod. 90 (4), 365–378. http://dx.doi.org/10.1007/s00190-015-0878-1.

Lyard, F., Lefevre, F., Letellier, T., Francis, O., 2006. Modelling the global ocean tides: modern insights from FES2004. Ocean Dynam. 56 (5–6), 394–415. http://dx.doi.org/10.1007/s10236-006-0086-x.

Meindl, M., Schaer, S., Dach, R., Beutler, G., 2011. Different reference frame realizations using data from a global network of multi-GNSS receivers. In: Proc. 3rd Int. Coll. on Scientific and Fundamental Aspects of the Galileo Program, Copenhagen.

Meindl, M., Beutler, G., Thaller, D., et al., 2013. Geocenter coordinates estimated from GNSS data as viewed by perturbation theory. Adv. Space Res. 51 (7), 1047–1064. http://dx.doi.org/10.1016/j.asr.2012.10.026.

Montenbruck, O., Hauschild, A., 2013. Code biases in multi-GNSS point positioning. In: ION ITM 2013, pp. 616–628.

Montenbruck, O., Steigenberger, P., 2016. Multi-GNSS Working Group Technical Report 2015. In: Jean, Y., Dach, R. (Eds.), IGS Technical Report 2015, University of Bern, pp. 173–182. http://dx.doi.org/10.7892/boris.80307.

Montenbruck, O., Hauschild, A., Hessels, U., et al., 2009. CONGO – first GPS/GIOVE tracking network for science, research. GPS World 20 (9), 56–62.

Montenbruck, O., Hauschild, A., Hessels, U., 2011. Characterization of GPS/GIOVE sensor stations in the CONGO network. GPS Solut. 15 (3), 193–205. http://dx.doi.org/10.1007/s10291-010-0182-8.

Montenbruck, O., Steigenberger, P., Schönemann, E., et al., 2012a. Flight characterization of new generation GNSS satellite clocks. Navigation 59 (4), 291–302. http://dx.doi.org/10.1002/navi.22.

Montenbruck, O., Hugentobler, U., Dach, R., et al., 2012b. Apparent clock variations of the Block IIF-1 (SVN62) GPS satellite. GPS Solut. 16 (3), 303–313. http://dx.doi.org/10.1007/s10291-011-0232-x.

Montenbruck, O., Hauschild, A., Steigenberger, P., 2014. Differential code bias estimation using multi-GNSS observations and global ionosphere maps. Navigation 61 (3), 191–201. http://dx.doi.org/10.1002/navi.64.

Montenbruck, O., Steigenberger, P., Hauschild, A., 2015a. Broadcast versus precise ephemerides: a multi-GNSS perspective. GPS Solut. 19 (2), 321–333. http://dx.doi.org/10.1007/s10291-014-0390-8.

Montenbruck, O., Schmid, R., Mercier, F., et al., 2015b. GNSS satellite geometry and attitude models. Adv. Space Res. 56 (6), 1015–1029. http://dx.doi.org/10.1016/j.asr.2015.06.019.

Montenbruck, O., Steigenberger, P., Hugentobler, U., 2015c. Enhanced solar radiation pressure modeling for Galileo satellites. J. Geod. 89 (3), 283–297. http://dx.doi.org/10.1007/s00190-014-0774-0.

Montenbruck, O., Steigenberger, P., Riley, S., 2015d. IRNSS Orbit Determination and Broadcast Ephemeris Assessment. In: ION ITM 2015, 185–193.

Nadarajah, N., Teunissen, P.J.G., Sleewaegen, J.-M., Montenbruck, O., 2015. The mixed-receiver BeiDou inter-satellite-type bias and its impact on RTK positioning. GPS Solut. 19 (3), 357–368. http://dx.doi.org/10.1007/s10291-014-0392-6.

Noll, C.E., 2010. The Crustal Dynamics Data Information System: a resource to support scientific analysis using space geodesy. Adv. Space Res. 45 (12), 1421–1440. http://dx.doi.org/10.1016/j.asr.2010.01.018.

Odijk, D., Teunissen, P.J.G., 2013. Estimation of differential inter-system biases between the overlapping frequencies of GPS, Galileo, BeiDou and QZSS. In: Proc. 4th Int. Coll. Scientific and Fundamental Aspects of the Galileo Programme, Prague, ESA.

Odijk, D., Nadarajah, N., Zaminpardaz, S., Teunissen, P.J.G., 2016. GPS, Galileo, QZSS and IRNSS differential ISBs: estimation and application. GPS Solut. http://dx.doi.org/10.1007/s10291-016-0536-y.

Pavlis, E.C., 2009. SLRF2008: The ILRS reference frame for SLR POD contributed to ITRF2008. In: 2009 Ocean Surface Topography Science Team Meeting, Seattle.

Paziewski, J., Wielgosz, P., 2015. Accounting for Galileo–GPS inter-system biases in precise satellite positioning. J. Geod. 89 (1), 81–93. http://dx.doi.org/10.1007/s00190-014-0763-3.

Paziewski, J., Sieradzki, R., Wielgosz, P., 2015. Selected properties of GPS and Galileo-IOV receiver intersystem biases in multi-GNSS data processing. Meas. Sci. Technol. 26 (9), 095008. http://dx.doi.org/10.1088/0957-0233/26/9/095008.

Pearlman, M.R., Degnan, J.J., Bosworth, J.M., 2002. The international laser ranging service. Adv. Space Res. 30 (2), 135–143. http://dx.doi.org/10.1016/S0273-1177(02)00277-6.

Prange, L., Dach, R., Lutz, S., et al., 2016a. The CODE MGEX orbit and clock solution. In: Rizos, C., Willis, P. (Eds.), IAG 150 Years, International Association of Geodesy Symposia, vol. 143. Springer, pp. 767–773. http://dx.doi.org/10.1007/1345_2015_161.

Prange, L., Orliac, E., Dach, R., et al., 2016b. CODE's five-system orbit and clock solution – the challenges of multi-GNSS data analyis. J. Geod. http://dx.doi.org/10.1007/s00190-016-0968-8.

Ray, J., Gurtner, W., 2010. RINEX Extensions to Handle Clock Information, Version 3.02. <https://igscb.jpl.nasa.gov/igscb/data/format/rinex_clock302.txt>.

Rebischung, P., Altamimi, Z., Ray, J., Garayt, B., 2016. The IGS contribution to ITRF2014. J. Geod. 90 (7), 611–630, ISSN 1432-139. http://dx.doi.org/10.1007/s00190-016-0897-6.

Rodriguez-Solano, C.J., 2014. Impact of non-conservative force modeling on GNSS satellite orbits and global solutions (Ph.D. thesis). Technische Universität München.

Rodriguez-Solano, C.J., Hugentobler, U., Steigenberger, P., 2012a. Adjustable box-wing model for solar radiation pressure impacting GPS satellites. Adv. Space Res. 49 (7), 1113–1128. http://dx.doi.org/10.1016/j.asr.2012.01.01.

Rodriguez-Solano, C., Hugentobler, U., Steigenberger, P., 2012b. Impact of albedo radiation on GPS satellites. In: Geodesy for Planet Earth. International Association of Geodesy Symposia, vol. 136. Springer, pp. 113–119. http://dx.doi.org/10.1007/978-3-642-20338-1_14.

Rodriguez-Solano, C.J., Hugentobler, U., Steigenberger, P., et al., 2014. Reducing the draconitic errors in GNSS geodetic products. J. Geod. 88 (6), 559–574. http://dx.doi.org/10.1007/s00190-014-0704-1.

Rothacher, M., Schmid, R., ANTEX: the antenna exchange format, Version 1.4, 15 Sep 2010. <ftp://igs.org/pub/station/general/antex14.txt>.

Rothacher, M., Thaller, D., 2006. SINEX – Solution (Software/technique) INdependent EXchange Format Version 2.02, 1 December 2006. <https://www.iers.org/SharedDocs/Publikationen/EN/IERS/Documents/ac/sinex/sinex_v202_pdf>.

RTCM, 2016. Radio Technical Commission for Maritime Services (RTCM) Standard 10403.3, Differential GNSS (Global Navigation Satellite Systems) Services, Version 3, 7 Oct. 2016.

Schaer, S., 2016. SINEX_BIAS - Solution (Software/technique) INdependent EXchange Format for GNSS Biases, Draft Version 1.00, July 2016. <http://www.aiub.unibe.ch/download/bcwg/format/draft/sinex_bias_100.pdf>.

Schmid, R., Dach, R., Collilieux, X., et al., 2016. Absolute IGS antenna phase center model igs08.atx: status and potential improvements. J. Geod. 90 (4), 343–364. http://dx.doi.org/10.1007/s00190-015-0876-3.

Schmitz, M., Wübbena, G., Boettcher, G., 2002. Tests of phase center variations of various GPS antennas, and some results. GPS Solut. 6 (1–2), 18–27. http://dx.doi.org/10.1007/s10291-002-0008-4.

Simsky, A., 2006. Three's the charm: triple-frequency combinations in future GNSS. Inside GNSS 1 (5), 38–41.

Soehne, W., Mervart, L., Ruelke, A., et al., 2015. Quality checking for multi-GNSS data. In: Geophys. Res. Abstr., vol. 17, EGU2015-1895-1.

Sośnica, K., Thaller, D., Dach, R., et al., 2015. Satellite laser ranging to GPS and GLONASS. J. Geod. 89 (7), 725–743. http://dx.doi.org/10.1007/s00190-015-0810-8.

Springer, T., 2011. SINEX_BIAS - Solution (Software/technique) INdependent EXchange Format for GNSS Biases Version 0.01 (June 29, 2011). <http://www.biasws2012.unibe.ch/docs/sinex_bias_0.01-2.txt>.

Steigenberger, P., Montenbruck, O., 2016. Galileo status: orbits, clocks, and positioning. GPS Solut. http://dx.doi.org/10.1007/s10291-016-0566-5.

Steigenberger, P., Hugentobler, U., Montenbruck, O., Hauschild, A., 2011. Precise orbit determination of GIOVE-B based on the CONGO network. J. Geod. 85 (6), 357–365. http://dx.doi.org/10.1007/s00190-011-0443-5.

Steigenberger, P., Hugentobler, U., Hauschild, A., Montenbruck, O., 2013. Orbit and clock analysis of Compass GEO and IGSO satellites. J. Geod. 87 (6), 515–525. http://dx.doi.org/10.1007/s00190-013-0625-4.

Steigenberger, P., Montenbruck, O., Hessels, U., 2015a. Performance evaluation of the early CNAV navigation message. Navigation 62 (3), 219–228. http://dx.doi.org/10.1002/navi.111.

Steigenberger, P., Hugentobler, U., Loyer, S., et al., 2015b. Galileo orbit and clock quality of the IGS Multi-GNSS Experiment. Adv. Space Res. 55 (1), 269–281. http://dx.doi.org/10.1016/j.asr.2014.06.030.

Steigenberger, P., Montenbruck, O., Hugentobler, U., 2015c. GIOVE-B solar radiation pressure modeling for precise orbit determination. Adv. Space Res. 55 (5), 1422–1431. http://dx.doi.org/10.1016/j.asr.2014.12.009.

Steigenberger, P., Fritsche, M., Dach, R., et al., 2016. Estimation of satellite antenna phase center offsets for Galileo. J. Geod. 90 (8), 773–785. http://dx.doi.org/10.1007/s00190-016-0909-6.

Sun, B., Su, H., Zhang, Z., et al., 2016. GNSS GEO satellites precise orbit determination based on carrier phase and SLR observations. In: IGS Workshop 2016, Sydney.

Tan, B., Yuan, Y., Wen, M., et al., 2016. Initial results of the precise orbit determination for the new-generation BeiDou satellites (BeiDou-3) based on the iGMAS network. ISPRS Int. J. Geo-Inform. 5 (11), 196. http://dx.doi.org/10.3390/ijgi5110196.

Tang, W., Deng, C., Shi, C., Liu, J., 2014. Triple-frequency carrier ambiguity resolution for Beidou navigation satellite system. GPS Solut. 18 (3), 335–344. http://dx.doi.org/10.1007/s10291-013-0333-9.

Tegedor, J., Øvstedal, O., 2014. Triple carrier precise point positioning (PPP) using GPS L5. Surv. Rev. 46 (337), 288–297. http://dx.doi.org/10.1179/1752270613Y.0000000076.

Tegedor, J., Øvstedal, O., Vigen, E., 2014. Precise orbit determination and point positioning using GPS, Glonass, Galileo and BeiDou. J. Geod. Sci. 4 (1), 65–73. http://dx.doi.org/10.2478/jogs-2014-0008.

Teunissen, P., Joosten, P., Tiberius, C., 2002. A comparison of TCAR, CIR and LAMBDA GNSS ambiguity resolution. In: ION GPS 2002, pp. 2799–2808.

Uhlemann, M., Gendt, G., Ramatschi, M., Deng, Z., 2016. GFZ global multi-GNSS network and data processing results. In: Rizos, C., Willis, P. (Eds.), IAG 150 Years, International Association of Geodesy Symposia, vol. 143. Springer, pp. 673–679. http://dx.doi.org/10.1007/1345_2015_120.

Urlichich,Y., Subbotin, V., Stupak, G., et al., GLONASS modernization. In: ION GNSS+ 2011, pp. 3125–3128.

Vaclavovic, P., Dousa, J., 2015. G-Nut/Anubis: open-source tool for multi-GNSS data monitoring with a multipath detection for new signals, frequencies and constellations. In: Rizos, C., Willis, P. (Eds.), IAG 150 Years, International Association of Geodesy Symposia, vol. 143. Springer, pp. 775–782,. http://dx.doi.org/10.1007/1345_2015_97.

Vergara, M., Sgammini, M., Thoelert, S., et al., 2016. Tracking error modeling in presence of satellite imperfections. Navigation 63 (1), 3–13. http://dx.doi.org/10.1002/navi.129.

Wang, K., Rothacher, M., 2013. Ambiguity resolution for triple-frequency geometry-free and ionosphere-free combination tested with real data. J. Geod. 87 (6), 539–553. http://dx.doi.org/10.1007/s00190-013-0630-7.

Wang, G., de Jong, K., Zhao, Q., et al., 2015. Multipath analysis of code measurements for BeiDou geostationary satellites. GPS Solut. 19 (1), 129–139. http://dx.doi.org/10.1007/s10291-014-0374-8.

Wang, B., Lou, Y., Liu, J., et al., 2016a. Analysis of BDS satellite clocks in orbit. GPS Solut. 20 (4), 783–794. http://dx.doi.org/10.1007/s10291-015-0488-7.

Wang, N., Yuan, Y., Li, Z., et al., 2016b. Determination of differential code biases with multi-GNSS observations. J. Geod. 90 (3), 209–228. http://dx.doi.org/10.1007/s00190-015-0867-4.

Wanninger, L., Beer, S., 2015. BeiDou satellite-induced code pseudorange variations: diagnosis and therapy. GPS Solut. 19 (4), 639–648. http://dx.doi.org/10.1007/s10291-014-0423-3.

Weber, R., Slater, J.A., Fragner, E., et al., 2005a. Precise GLONASS orbit determination within the IGS/IGLOS – pilot project. Adv. Space Res. 36 (3), 369–375. http://dx.doi.org/10.1016/j.asr.2005.08.051.

Weber, G., Dettmering, D., Gebhard, H., Kalafus, R., 2005b. Networked transport of RTCM via Internet Protocol (Ntrip) – IP-streaming for real-time GNSS applications. In: ION GNSS 2005, pp. 2243–2247.

Weber, G., Hauschild, A., Stöcker, D., et al., 2011. Real-time PPP based on CONGO and RTCM's multiple signal messages. In: Geophy. Res. Abstr., vol. 13, EGU2011-10970.

Weber, G., Mervart, L., Stürze, A., et al., 2016. BKG Ntrip Client (BNC) version 2.12, Mitteilungen des Bundesamtes für Kartographie und Geodäsie, vol. 49.

Wermuth, M., Montenbruck, O., van Helleputte, T., 2010. GPS High Precision Orbit Determination Software Tools (GHOST). In: 4th International Conference on Astrodynamics Tools and Techniques, Madrid.

Willis, P., Beutler, G., Gurtner, W., et al., 1999. IGEX: international GLONASS experiment – scientific objectives and preparation. Adv. Space Res. 23 (4), 659–663. http://dx.doi.org/10.1016/S0273-1177(99)00147-7.

Xiao, W., Liu, W., Sun, G., 2016. Modernization milestone: BeiDou M2-S initial signal analysis. GPS Solut. 20 (1), 125–133. http://dx.doi.org/10.1007/s10291-015-0496-7.

Xue, J., Song, S., Liao, X., Zhu, W., 2016a. Estimating and assessing Galileo navigation system satellite and receiver differential code biases using the ionospheric parameter and differential code bias joint estimation approach with multi-GNSS observations. Radio Sci. 51 (4), 271–283. http://dx.doi.org/10.1002/2015RS005797.

Xue, J., Song, S., Zhu, W., 2016b. Estimation of differential code biases for Beidou navigation system using multi-GNSS observations: how stable are the differential satellite and receiver code biases? J. Geod. 90 (4), 309–321. http://dx.doi.org/10.1007/s00190-015-0874-5.

Yang, Y., Li, J., Wang, A., et al., 2014. Preliminary assessment of the navigation and positioning performance of BeiDou regional navigation satellite system. Sci. China Earth Sci. 57 (1), 144–152. http://dx.doi.org/10.1007/s11430-013-4769-0.

Yinger, C.H., Feess, W.A., Di Esposti, R., et al., 1999. GPS satellite interfrequency biases. In: ION-AM 1999, pp. 347–354.

Yudanov, S., 2013. Signal decoding with conventional receiver and antenna – a case history using the New Galileo E6-B/C signal. GPS World 24 (2), 34–37.

Zaminpardaz, S., Teunissen, P.J.G., Nadarajah, N., 2016. GLONASS CDMA L3 ambiguity resolution and positioning. GPS Solut. http://dx.doi.org/10.1007/s10291-016-0544-y.

Zhao, Q., Chen, G., Guo, J., Liu, J., 2016. A priori solar radiation pressure model for QZSS Michibiki satellite. In: IGS Workshop 2016, Sydney.

Ziebart, M., Adhya, S., Sibthorpe, A., et al., 2005. Combined radiation pressure and thermal modelling of complex satellites: algorithms and on-orbit tests. Adv. Space Res. 36 (3), 424–430. http://dx.doi.org/10.1016/j.asr.2005.01.014.